Per. Mineral. (1999), *68*, 2, 185-212

PERIODICO di MINERALOGIA
established in 1930

An International Journal of
MINERALOGY, CRYSTALLOGRAPHY, GEOCHEMISTRY, ORE DEPOSITS, PETROLOGY, VOLCANOLOGY
and applied topics on *Environment, Archaeometry* and *Cultural Heritage*

Geological and geochemical characteristics of Permian tourmalinization at Val Trompia (southern Alps, northern Italy) and relationship with the Orobic tourmalinites

LUISA DE CAPITANI[1], MARILENA MORONI[1*] and FRANCO RODEGHIERO[2]

[1] Dipartimento di Scienza della Terra, Università di Milano, Via Botticelli 23, I-20133 Milano, Italy
[2] Dipartimento di Georisorse e Territorio, Politecnico di Torino, Corso Duca degli Abruzzi 24, I-10129 Torino, Italy

Submitted December 1998 - Accepted May 1999

ABSTRACT. — Tourmaline breccias in the pre-Alpine basement in Val Trompia (Southern Alps, Northern Italy) are related to late Palaeozoic granites and are associated with Sn-W-bearing ore deposits. The breccias are rich in acicular tourmaline with variable textural and compositional characteristics. At least four stages of tourmaline crystallization are distinguished, mainly by Mg/Fe ratios. All tourmalines can be classified as «alkali group» varieties using recent nomenclature schemes. Compositions vary from schorl-dravite for earlier, main-stage type I and II coarse crystals, to highly Fe-enriched tourmalines, probably approaching the povondraite endmember (typical of oxidized hydrothermal environments), for type III and IV fine-grained tourmalines within late veinlets. Whole-rock REE geochemical data show variable, locally remarkable enrichments in LREE related to the action of hydrothermal fluids. Coarse tourmalines occurring in the cryptocrystalline groundmass of the Orobic tourmalinites, which are hosted in cataclastic zones along the tectonic contact between basement and Permian volcano-sedimentary cover rocks in the Lake Diavolo area (southern Alps), have schorl-dravite compositions similar to type I and II, main-stage Val Trompia tourmalines. The Orobic tourmalinites were considered of metasomatic origin by previous studies.

The Val Trompia tourmalinites can be interpreted as having formed by magmatic-hydrothermal fluids that produced metasomatic tourmalines with different compositions at different distances from the fluid source (magma). Compositional analogies between tourmalinites of the two areas may therefore reflect similarities between the tourmalinization processes that developed in relation to large-scale Permian magmatic-tectonic activity. The Val Trompia tourmalinites thus may represent deeper metasomatic products, closer to the magma chamber, whereas the Orobic tourmalinites would have formed from hydrothermal fluids injected along shallower faults during coeval volcanic activity.

RIASSUNTO. — Brecce a tormalina affioranti nel basamento sudalpino in Val Trompia, in relazione con lineamenti e granitoidi tardo-paleozoici ed associate a mineralizzazioni a Sn e W, sono caratterizzate da tormaline con caratteri tessiturali e composizionali variabili. Tormaline appartenenti ad almeno quattro stadi genetici sono riconoscibili principalmente dalla variazione del rapporto Mg/Fe. Tutte le tormaline sono definibili come «alkali group tourmalines», in accordo con la più recente classificazione. La composizione varia da termini della serie schorlite-dravite, per i cristalli riferibili agli stadi di cristallizzazione più antichi (tipo I e II), fino a quelli estremamente arricchiti in Fe affini al termine povondraitico (tipico di ambiente idrotermale ossidato), per tormaline entro vene tardive (tipo III e IV). Dati relativi alle

* Corresponding author,
E-mail: marilena@r10.terra.unimi.it

terre rare su roccia totale mostrano arricchimenti variabili, talora notevoli di terre rare leggere, probabilmente legati all'azione di fluidi idrotermali. Sono state analizzate anche le tormaline di maggiori dimensioni nelle tormaliniti criptocristalline affioranti entro fasce cataclasitiche al contatto tra basamento e copertura vulcano-sedimentaria permiana nella zona del Lago del Diavolo (Alpi Orobie), già precedentemente definite di origine metasomatica. Queste tormaline ricadono nel campo composizionale della serie schorlite-dravite e sono analoghe a quelle trumpline di tipo I e II, la cui formazione è attribuita all'evento principale di tormalinizzazione, fortemente influenzato dal chimismo della roccia originaria. Le tormaliniti della Val Trompia sono interpretabili come originate da fluidi magmatico-idrotermali che, a distanze differenti dalla sorgente, per reazione metasomatica hanno prodotto tormaline di differente composizione. Analogie composizionali tra le tormaliniti delle due aree sembrano quindi riflettere una somiglianza tra i processi di tormalinizzazione avvenuti su larga scala e legati all'attività magmato-tettonica permiana. In questo ambito le tormaliniti della Val Trompia potrebbero rappresentare i prodotti metasomatici di maggior profondità, in prossimità della camera magmatica, mentre quelle orobiche rappresenterebbero il prodotto legato ai fluidi, convogliati lungo sistemi di fratture, che alimentavano il vulcanismo superficiale.

KEY WORDS: *Southern Alps, Permian, tourmaline chemistry, tourmalinite, boron metasomatism.*

INTRODUCTION

Tourmalines and tourmaline-rich rocks occur in direct and indirect association with a variety of geologic environments and ore deposits of diverse age, as summarized extensively in the recent volume on boron edited by the Mineralogical Society of America (Grew and Anovitz, 1996).

Due to its complex chemical nature, tourmaline is known to acquire a specific compositional signature according to different conditions of crystallization. Therefore tourmaline represents a valuable tool for evaluating the geochemistry of a mineralizing environment and may be an important pathfinder for ore deposits. This work investigates for the first time the geological and geochemical characteristics of tourmaline-rich breccia rocks recently found in Val Trompia (central southern Alps, northern Italy). There, Alpine compressive tectonics only partly concealed late Palaeozoic geological and structural elements belonging to the post-Variscan rifting, which greatly influenced the geology and metallogeny of the entire southern Alpine domain in northern Italy. Val Trompia tourmalinites show textural complexities and spatial relationships to late Palaeozoic lineaments, magmatic rocks, and ore deposits. For these reasons they have been studied in detail in order to evaluate their compositional variability and gain insights into their genesis. These tourmalinites are further compared with tourmaline-rich rocks of metasomatic origin hosted by Permian palaeo-faults (Zhang *et al.*, 1994; Slack *et al.*, 1996) and those geologically related to the Permian boron-bearing U mineralization at Novazza and Val Vedello in the central Orobic Alps (Fuchs and Maury, 1995). An attempt is also made to construct a model relating the Val Trompia and Orobic tourmalinizations to the late Palaeozoic geologic and metallogenic framework of the central southern Alps.

REGIONAL GEOLOGY

The areas of Val Trompia and of Lake Diavolo-Lake Publino (indicated below as Lake Diavolo in short) are located in Lombardy (Northern Italy) and belong to the central sector of the South Alpine domain (fig.1).

The Val Trompia area (labelled 1 in fig. 1; fig. 2) includes the southernmost exposure of the pre-Alpine crystalline basement: it consists of a small crystalline massif 3-4 km wide that crops out for about 15 km in a ENE-WSW direction. The Lake Diavolo area (labelled 2 in fig. 1; fig. 4) is at the southern margin of the central part of the wide Orobic Massif (Orobic Alps), exposed with continuity over a distance of more than 100 km in a E-W direction from the Insubric Line southwards.

The main structure of the region reflects the

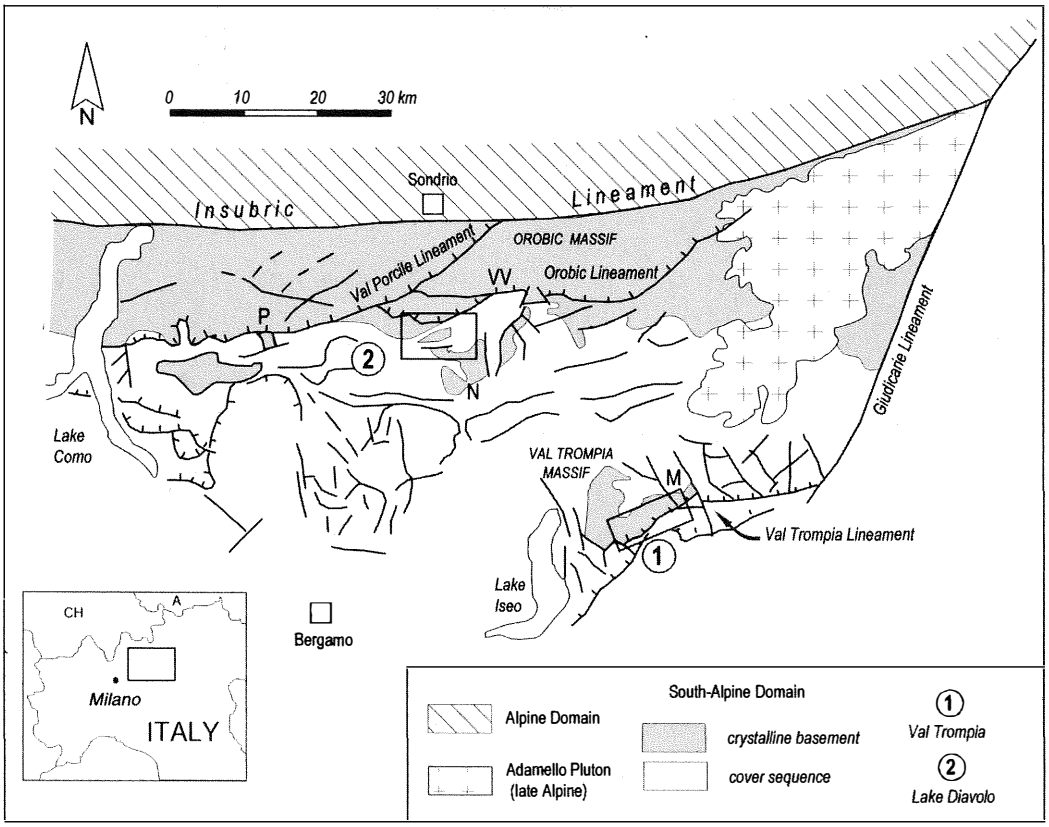

Fig. 1 – Simplified regional geological sketch map of the central sector of the South Alpine domain showing relative distribution of Variscan basement and post-Variscan cover, main tectonic lineaments, and the two study areas of Val Trompia (area 1) and Lake Diavolo-Lake Publino (area 2). Labels: P: Lake Pescegallo; VV: Val Vedello; N: Novazza; M: Maniva Pass-Val di Vaia.

complex tectonic relationships between the pre-Alpine, Variscan basement and post-Variscan, upper Palaeozoic-Lower Triassic volcano-sedimentary cover sequence.

Major tectonic lineaments show two main structural trends: E-W («Orobic» trend) and NNE-SSW («Giudicarie» trend). The Insubric, the Orobic, and the Val Trompia lineaments belong to the first trend. The second trend is named after the Giudicarie Lineament, which connects the «Orobic»-type Val Trompia Lineament and the Insubric Lineament to the north, and limits extension of the pre-Alpine basement to the east (fig. 1). Along these lineaments thrusting of the basement onto the post-Variscan cover sequence occurred during the Alpine orogeny. However, during upper Palaeozoic time several of these lineaments were already active as transtensional faults. They controlled development of the so-called «Collio Basin» *s.l.*, a major E-W-trending volcano-tectonic strike-slip and pull-apart basin system, consisting of a series of E-W-trending asymmetric graben basins (Orobic Basin, Boario Basin, Collio Basin *s.s.*, etc.) separated by basement horsts (Cassinis, 1985; Cassinis and Perotti, 1993; Cadel *et al.*, 1996). The regional Collio basin represents a phase of crustal thinning related to a continental-scale, left-lateral strike-slip displacement along the

palaeo-Insubric fault system that dismembered the Variscan collisional belt.

In both areas the basement shows a dominant retrogressive greenschist-facies metamorphic imprint of Variscan age, consisting of metasediments (phyllite and paragneiss) with minor amphibolite and marble intercalations (the latter in the Orobic basement only), and orthogneissic units (Giobbi Origoni and Gregnanin, 1983; Diella *et al.*, 1992; Cadel *et al.*, 1996; Gosso *et al.*, 1997). In the whole region the upper Palaeozoic-Lower Triassic volcano-sedimentary cover sequence filling the Permian tectonic basins is characterized by basal Upper Carboniferous-Lower Permian continental, alluvial to lacustrine terrigenous sediments (conglomerates, sandstones, slates) associated with abundant felsic volcanics and volcaniclastic deposits (Basal Conglomerate, Collio Fm.), overlain by Upper Permian continental, red bed-type sandstones and conglomerates of the Verrucano Lombardo Formation (Cassinis, 1985; Ori *et al.*, 1986; Cadel *et al.*, 1996). Stratigraphically above the Verrucano conglomerates, shallow-water limestones and marls (Servino Fm.) mark the Lower Triassic marine transgression leading to the opening of the Jurassic Tethys Ocean.

The highly active magmatism in the Carboniferous-Permian basins is recorded by widespread caldera-type volcanism and coeval plutonic to subvolcanic intrusions of magma with silicic to intermediate-basic compositions.

Evidence of hydrothermal activity and mineralization related to the Carboniferous-Permian geological and structural setting are also widespread in the region. Two major mineralized systems stand out. The Novazza-Val Vedello district, in the central-eastern Orobic Chain, is the largest hydrothermal uranium field in Italy, consisting of Permian fault-related uranium orebodies hosted in volcanic rocks of the Collio Formation (Cadel, 1986; Cadel *et al.*, 1987; Fuchs and Maury, 1995). The Val Trompia district, to the southeast, includes major swarms of siderite-sulphide-quartz veins (and associated Sn-W greisens), the Torgola fluorite vein system and the large Maniva Pass-Val di Vaia quartz-only vein system (indicated by M in fig. 1), all of which are in spatial relationship to upper Palaeozoic granitoid intrusions or faults (Frizzo, 1997; Moroni, 1994; Cassinis *et al.*, 1997).

VAL TROMPIA TOURMALINITES

Geological setting

In Val Trompia tourmalinite occurrences (fig. 2) are closely associated with the Val Trompia Lineament (VTL) along the southern margin of the crystalline massif, and with the distribution of both pre-Alpine magmatic and hydrothermal rocks. The palaeo-VTL, active during Permian time (Cassinis and Perotti, 1993), underwent Alpine reactivation by south-directed fragile reverse faulting and thrusting with limited deformational imprint on the pre-Alpine structures and units. Along the VTL phyllites are in tectonic contact with Permian and Lower Triassic strata, except along tracts near Bovegno and Graticelle where basement rocks crop out on both sides of the thrust plane and relationships with the cover units are governed by swarms of faults conformable to the VLT trend.

Pre-Alpine magmatic rocks also are closely related to the VTL. Upper Palaeozoic silicic volcanics of the Collio Formation occur extensively in the northeastern part of the region, near the intersection of the VTL and the Giudicarie Line (fig. 1), an area where the Collio Formation crops out extensively and that represents a major center of volcanic activity feeding one of the main depocenters of the Collio basin (Cassinis and Perotti, 1993).

Plutonic rocks are sparsely exposed along the central and western sector of the VTL: the Val Torgola-Val Navazze (shortened to Torgola) K-Al-rich granite complex (outcropping near Graticelle location; fig. 2) and the Val Cavallina mildly alkaline gabbro stock (to the west of the study area; De Capitani and Moroni, 1992). Other intrusives, the Val di Rango quartz-diorite and the Maniva Pass Al-rich granodiorite (Mora, 1992), occur to the

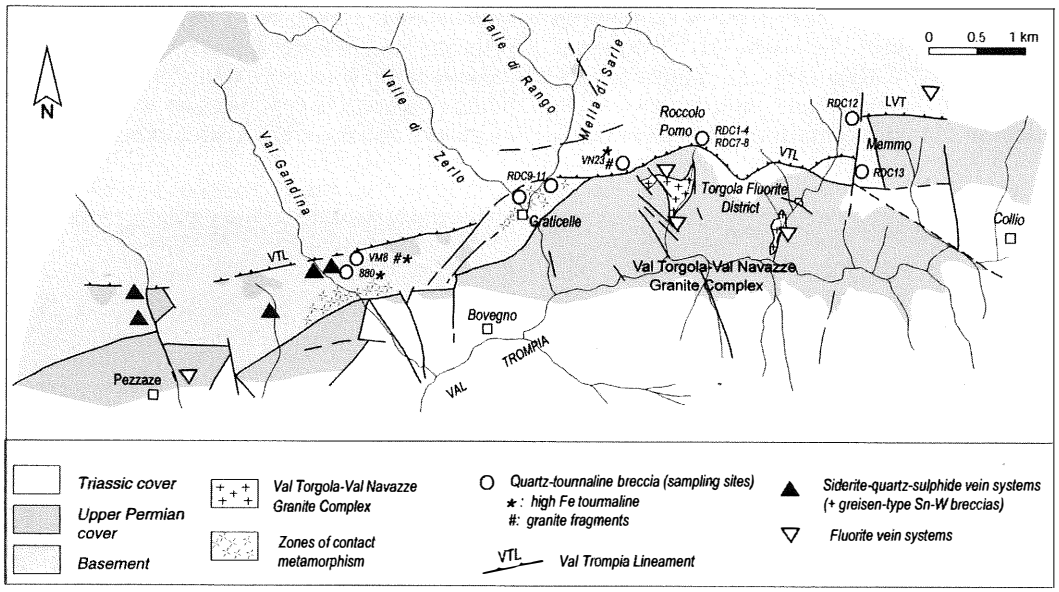

Fig. 2 – Schematic geological map of the central Val Trompia area showing distribution of the tourmaline breccia bodies relative to the reactivated Val Trompia Lineament, mineralized vein systems, outcropping granitic rocks of the Val Torgola-Val Navazze granitoid complex, and zones of thermal metamorphism in basement phyllites.

north of the VTL, close to the unconformity between the basement and the upper Palaeozoic cover, at a short distance from the study area (close to M in fig. 1); tourmaline-bearing pegmatite veinlets are associated with the Maniva Pass granodiorite. All intrusives are post-kinematic relative to the main Variscan foliation (S_2) in the basement host rocks. The Torgola complex was eroded and covered by the Upper Permian Verrucano sandstones. A reliable, Rb-Sr isochron cooling age of 271+/–4 Ma was obtained only for the Torgola complex, which was emplaced at P-T conditions of ca. 1.5 kbar and 550°C (De Capitani *et al.*, 1994). Hence this intrusive complex appears to be broadly coeval with the Collio volcanics (approximate U/Pb zircon age of 280 Ma for Collio ignimbrites in the Orobic Alps and Val Trompia; in Philippe *et al.*, 1987) and may represent a portion of the magmatic chamber that fed Collio volcanism.

There is abundant evidence of pre-Alpine hydrothermal activity within the schists and the upper Palaeozoic cover units near the VTL. Some of the main deposits are shown in fig. 2; their distribution overlaps with that of the tourmalinites. North of Pezzaze and Bovegno, swarms of siderite-quartz-base metal sulfide veins, and associated greisen-type wolframite-scheelite-cassiterite breccias, occur along the southwestern margin of the crystalline massif close to the VTL and proximal to a zone of thermally metamorphosed sillimanite-andalusite-bearing schists suggesting the presence of the Val Torgola-Val Navazze granitoid complex at shallow depths to the west (Moroni, 1994). To the east, a large fluorite vein system (fig. 2) cuts the Torgola intrusive complex and the Upper Permian Verrucano conglomerates (Frizzo, 1997).

Field Relationships

Tourmaline-quartz breccia bodies (tourmalinites) represent an additional product of hydrothermal activity in the area; their

distribution closely follows the VTL trend in its central sector, between the villages of Pezzaze and Collio (fig. 2). Tourmalinite bodies cut the basement chlorite-muscovite phyllites and commonly form dm- to m-thick, fault-related, pseudo-concordant to discordant pods and veins of brecciated rock with a black microcrystalline groundmass. Typical is hydraulic breccia-type texture with whitish, angular, quartz-rich lithic, metamorphic

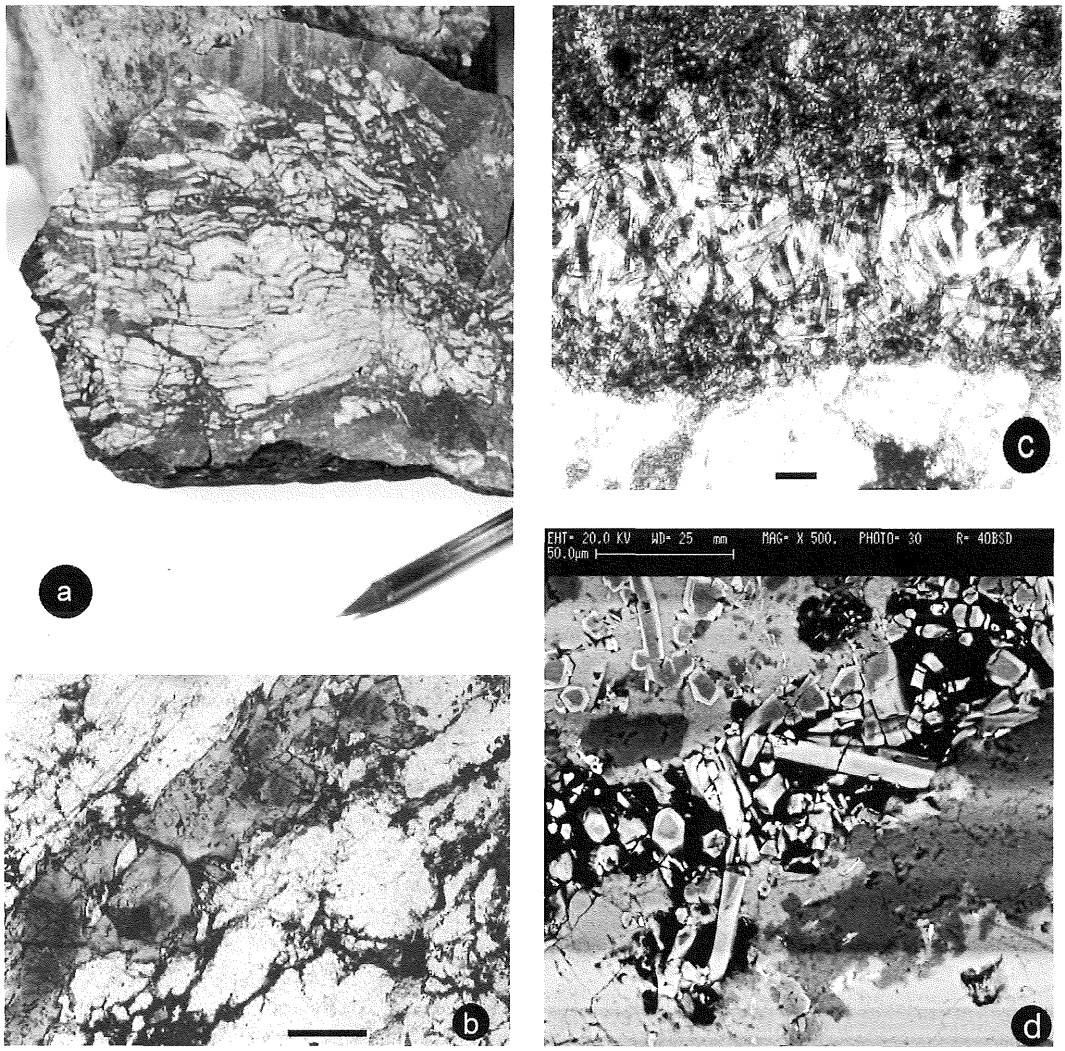

Fig. 3 – Val Trompia tourmalinites. *(a)* Fragment of paragneiss breccia affected by moderate tourmalinization; replacement by fine-grained, acicular tourmaline aggregated follows fractures and foliation planes; *(b)* coarse, prismatic, type II tourmaline crystal including remnants of darker, type I tourmaline in the core and hosted in quartz-rich matrix (sample RDC11; plane polarized light; scale bar is approximately 250 µm); *(c)* radiating aggregates of acicular, type III tourmaline crystals in the late quartz-tourmaline veinlets (sample 880; plane polarized light; scale bar is approximately 40 µm); (d) back scattered electron (BSE) image of the type IV tourmaline occurring as rims around cores of type III tourmaline in the late-stage veinlet shown in (c) (sample 880).

fragments (phyllite, quartzitic paragneiss) cemented and variably replaced by a felt-like groundmass of microcrystalline, acicular tourmaline. Thin quartz-tourmaline and younger quartz-only veinlets crosscut the breccia. Extreme tourmalinization locally has produced a black, massive, very hard rock in which the quartz fragments are almost completely replaced. In less tourmalinized facies, replacement by tourmaline commonly follows foliation planes of the schists (fig. 3*a*), mylonitic bands in strained quartzite levels and discordant fractures.

Near Roccolo Pomo (fig. 2), a large tourmalinite outcrop is located along the reactivated VTL, truncated and in part in direct contact with the Upper Permian Verrucano sandstones, which are not tourmalinized. Near Graticelle and west of Bovegno several tourmalinite bodies are near and above the zone of thermally metamorphosed phyllites, and in faults near the outcrops of the Pezzaze-Bovegno siderite-sulphide-quartz vein system. In both locations tourmalinites contain small, unaltered pieces of fine-grained leucogranite (consisting of euhedral albite and interstitial quartz), partly overgrown by the micro-crystalline aggregates of tourmaline. Fragments of fresh tourmalinite also occur in the greisen-type Sn-W breccia mineralization (Moroni, 1994).

Textures

At the micro-scale mineral components are dominated by micro-crystalline green to yellow tourmaline (average size about 10 μm) in dense felt-like aggregates, mosaic- and comb-textured vein quartz, polycrystalline quartz fragments of metamorphic origin (locally showing highly strained, mylonitic textures), sericite, abundant rutile, chlorite, and accessory oxidized pyrite.

By textural analysis four generations or types of tourmalines are distinguished. Yellow-green tourmaline (main stage or type II) is commonly in felt-like aggregates of microcrystalline, pale green, acicular tourmaline crystals with average size of about 10 μm, pervasively replacing the brecciated schists. Where tourmalinization is less intense, conformable overgrowths of type II tourmaline occur around metamorphic blue-green tourmaline crystals (type I) oriented along the foliation of the brecciated host schist. Rarely, aggregates of coarse (average diameter of about 100 μm), prismatic, type II yellow-pale green crystals stand out in the acicular groundmass and may preserve irregular type I cores (fig. 3*b*). The coarse type II tourmalines are weakly pleochroic and may show irregular, weak optical zoning commonly not related to compositional variations. Stockworks of quartz veinlets, rimmed by radiating aggregates of acicular (about 10 μm), deep green tourmaline (type III), generally cut the type II groundmass in the breccia (fig. 3*c*). These veinlets may be lined by thin selvedges of fine-grained, flaky, hydrothermal muscovite. In some samples (Pezzaze-Bovegno area, nearest the siderite veins) BSE images of the type III acicular crystals show the latest generation of tourmaline (type IV) occurring as very thin (2-3 μm) rims around more or less regular (fragmental) cores of type III tourmalines (fig. 3*d*). In most cases at least the first three types of tourmalines coexist in the same samples.

TOURMALINITES IN THE LAKE DIAVOLO AREA

Geological Setting

The tourmalinites at Lake Diavolo were first studied by Zhang *et al.* (1994) and Slack *et al.* (1996) from widespread, discontinuously tourmalinized Collio-basement contact zones («Orobic Tourmalinites» of Fuchs and Maury, 1995) extending from Lake Pescegallo in the west to Novazza and Val Vedello in the east (P, VV, and N in fig. 1).

In the Lake Diavolo area (fig. 4) a complex system of E-W-trending Alpine thrusts along reactivated Permian strike-slip faults gives way to a mutual tectonic overlapping between upper Palaeozoic cover and Variscan basement (dominated by orthogneisses of the Gneiss Chiari Fm.). The upper Palaeozoic units are here represented by discontinuous outcrops of

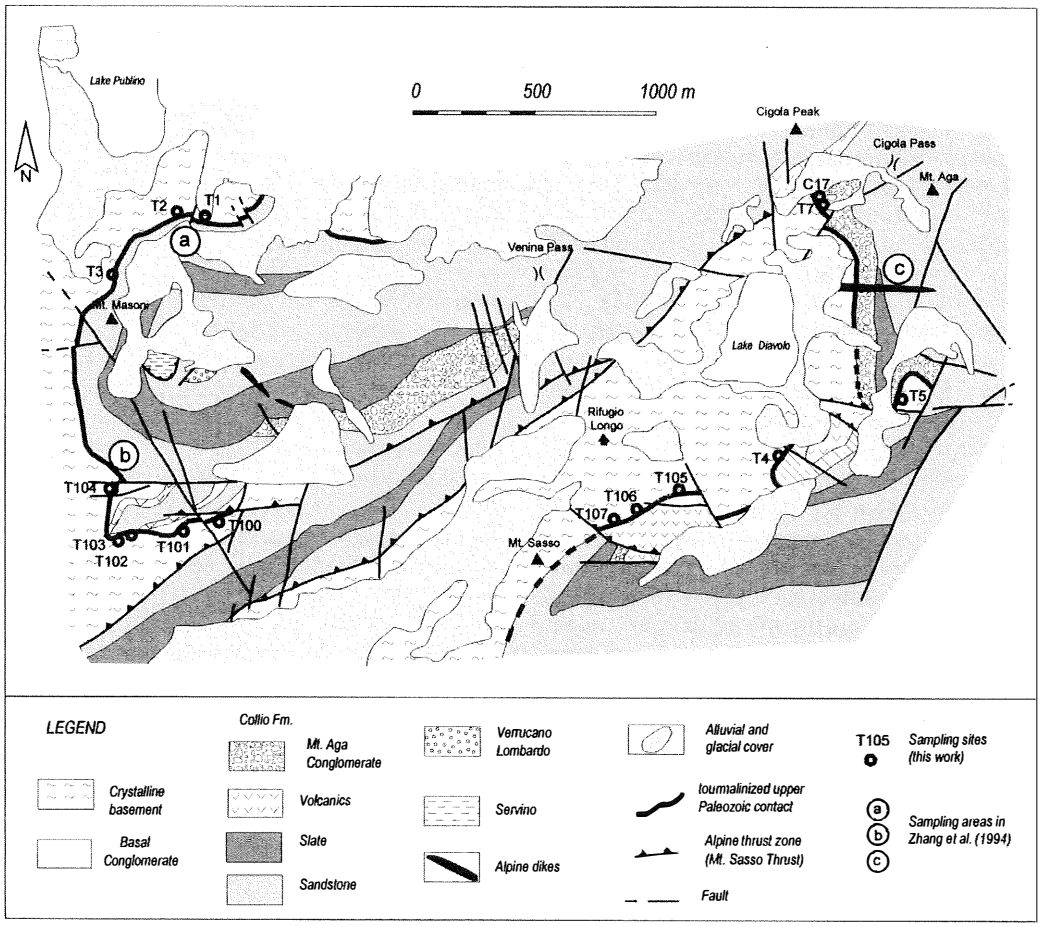

Fig. 4 – Schematic geological map of the Lake Diavolo-Lake Publino area in the central Orobic Alps (after Agazzi, 1997; D'Angiuro, 1997). Location of the sampling sites along the tourmalinized Permian contacts and approximate position of previous sampling zones labelled according to Zhang *et al.* (1994) are shown.

Basal Conglomerate, and by extensive exposures of the volcano-sedimentary Collio Formation, to which wedges of syn-sedimentary, fault-related debris are intercalated (Mount Aga Conglomerates) (Cadel *et al.*, 1996; Agazzi, 1997; D'Angiuro, 1997). Collio volcanic rocks (rhyolitic domes, tuffs, and ignimbrites) were erupted in several stages from a regional caldera-collapse structure extending ESE and ENE to the Novazza and Val Vedello mining areas, respectively (Cadel, 1986; Cadel *et al.*, 1987, 1996). No granitic intrusions coeval with the volcanic units are exposed in the area.

Tourmalinites are hosted by portions of the upper Palaeozoic fault system preserved by late reactivation and representing the original contact zone between basement orthogneisses with the cover units (Basal and Mount Aga Conglomerates, Collio sandstones, and volcaniclastic units) (fig. 4). These contact zones are believed to represent original, steep

décollements with an active escarpment towards the south along which alluvial sediments, volcanics, and fault-related debris flows were deposited. This upper Palaeozoic fault system was named the Mt. Masoni-Mt. Aga-Val Vedello Fault System by Cadel *et al.* (1996), and is also host to the Val Vedello-Novazza uranium district (Cadel, 1986; Cadel *et al.*, 1987).

The strong influence of the Alpine deformation on primary Permian structural features (tourmalinites included) is evidenced at various scales by km-scale upright folds with E-W axes, intense ductile shortening and localized formation of mylonitic zones accompanied by very low-grade metamorphism during southward-directed reverse faulting and thrusting (e.g., in fig. 4, Mt. Sasso Thrust, related to the Orobic Lineament) along the older, upper Palaeozoic basin-bounding faults (Cadel *et al.*, 1996). On the meso- and micro-scale, the ductile shortening is recorded in well developed crenulation and slaty cleavages and in a localized mylonitic foliation (Milano *et al.*, 1988; Zhang *et al.*, 1994; Cadel *et al.*, 1996). The contact zones hosting the tourmalinites are moderately disturbed by folding and affected by the Alpine cleavage.

In the study area contact-zone tourmalinites were sampled in detail, as indicated in fig. 4 (which also shows sampling sites of previous authors). Our sampling included cataclastic Mount Aga and Basal conglomerates along the contact zone, which contain quartz fragments rich in coarse tourmaline aggregates, either with undeformed vein-type or with foliated metamorphic textures (sampling sites T101 and C17, respectively, fig. 4).

Field Relationships and Textures

Tourmalinites occur as cm- to dm-sized, irregular bands and lenses of massive, black, aphanitic rock with rarely coarse, but more commonly ultra-cataclasite texture (fig. 5*a*). They are included in fault-rock (cataclasite) zones dm- to m-thick that affect the cover units (Basal and Mt. Aga conglomerates, Collio volcanics) and, to a lesser extent, basement orthogneiss (Zhang *et al.*, 1994). The tourmalinite zone is disrupted by late quartz veinlets and cut by the Alpine slaty cleavage with an angle of about 30° relative to the tourmalinite (fig. 5*a*). In the study area, the contact is characterized by a single, cm- to dm-thick, massive tourmalinized zone involving the Mt. Aga Conglomerate, or by multiple mm- to cm-thick, discontinuous lenses intermixed with cataclastic material at the contact with the Basal Conglomerate and Collio volcaniclastic rocks and sandstones. Faults and shear zones reactivated during Alpine time show often the development of mylonitic foliation and pseudotachylitic bands which can be mistaken with the tourmalinized zones. The discrimination between the two types was possible only by means of the analysis of the boron contents on bulk rock.

According to Zhang *et al.* (1994) the cryptocrystalline tourmalinite groundmass consists of over 70 vol% equant and extremely fine-grained (<0.02 μm) tourmaline crystals, with minor sheet silicates (probably clays) and quartz. Additional components are white mica (phengite; identified by X-ray diffraction), altered plagioclase, and rare pyrite and titanite. The cryptocrystalline groundmass commonly includes coarser subhedral to rounded tourmaline crystals with maximum size of about 50 μm (fig. 5*b*). Most of these tourmaline crystals are unzoned and light green, although locally some show a deep green colour and moderate pleochroism. These crystals locally exhibit thin recrystallized rims and phyllosilicate-bearing pressure shadows concordant with the Alpine cleavage; thus these tourmaline crystals were formed before the Alpine time and were affected by the Alpine deformation. Local coarser cataclastic textures reveal the metamorphic and volcanic nature of subangular lithic clasts, which can in some cases make up over 20 vol% of the rock.

As mentioned above, rock fragments in the Mount Aga and Basal conglomerates along the contact zone contain coarse tourmaline aggregates. The first type of tourmaline-bearing clasts in conglomerate consists of undeformed

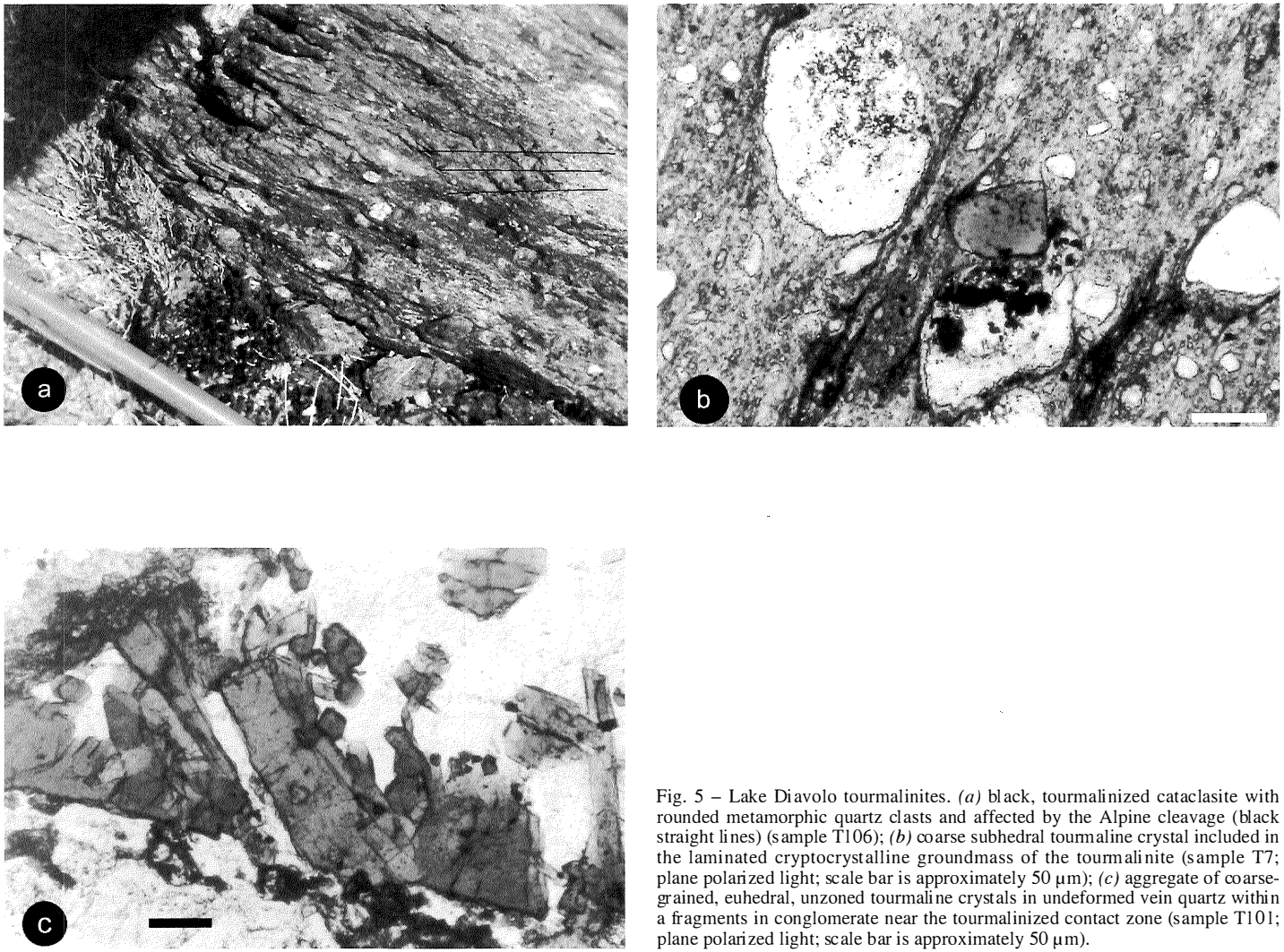

Fig. 5 – Lake Diavolo tourmalinites. *(a)* black, tourmalinized cataclasite with rounded metamorphic quartz clasts and affected by the Alpine cleavage (black straight lines) (sample T106); *(b)* coarse subhedral tourmaline crystal included in the laminated cryptocrystalline groundmass of the tourmalinite (sample T7; plane polarized light; scale bar is approximately 50 μm); *(c)* aggregate of coarse-grained, euhedral, unzoned tourmaline crystals in undeformed vein quartz within a fragments in conglomerate near the tourmalinized contact zone (sample T101; plane polarized light; scale bar is approximately 50 μm).

vein quartz and vuggy aggregates of euhedral, weakly pleochroic, unzoned, light green tourmaline crystals (fig. 5*c*). Fragments of metamorphic origin show thin lenses of strongly pleochroic, yellow to deep green tourmalines crystallized along foliation planes in the basement schist. These two types of coarse tourmalines are characterized by different compositional trends (see below). The tourmaline-bearing fragments are hosted in lithologies corresponding to coarse alluvial and debris flows related to the tectonic activity along the late-Palaeozoic boundary faults which have been tourmalinized. These different tourmaline-rich fragments may be useful in evaluating the nature of the coarse tourmaline grains in the contact-zone cryptocrystalline tourmalinites.

On chemical and geological grounds, Slack *et al.* (1996) compared the Lake Diavolo tourmalinites with the tourmaline-rich rocks occurring in the alteration envelope of the fault-hosted U mineralization in the Collio volcanics at Novazza (U-Pb and Pb-Pb dating of 249-240 Ma; in Cadel *et al.*, 1987). Slack *et al.* (1996) proposed a metasomatic origin and a Permian age for the Lake Diavolo tourmalinites.

Mineral and whole-rock chemistry

Analytical Methods

The chemical composition of the tourmalines was determined using an ARL-SEMQ electron microprobe. Operating conditions for the WDS method applied were 15 kV acceleration voltage, 20 nA beam current for all elements, and a 3 μm spot size. Some tourmalines were imaged with back scattered electrons (BSE) for better positioning of the spot on the surface of the smallest crystals (diameter <5 μm). Analytical data were corrected by the ZAF method. The following natural standards were used for calibration: corundum for Al, rhodonite for Mn, kaersutite for Si, Fe, Mg, Ca, Na, and K. Boron was not analyzed. Detection limits under the specified working conditions vary between 0.05 and 0.1 wt%. Some tourmalines from the Val Trompia samples were checked for F content under the following operating conditions: 15 kV acceleration voltage, 100 nA beam current, 10 μm spot size, and calibration on a synthetic fluorine-bearing standard.

Whole-rock chemical analyses of tourmaline-rich rocks were performed by X-ray fluorescence. Major, minor, and some trace elements, except the rare earth elements (REE), were determined on powder discs using an automated Philips PW 1400 spectrometer. Loss on ignition was determined on powders kept at 1000°C overnight. REE were determined by means of ICP-MS at C.R.P.G. (C.N.R.S.-Vandoeuvre lès Nancy, France) on selected samples from Val Trompia.

For the Orobic samples, X-ray powder diffraction allowed a preliminary discrimination between tourmaline-poor and tourmaline-rich lithologies. Boron concentrations of the latter samples were determined by graphite furnace-AAS on a Perkin Elmer 3030 Zeeman spectrometer. This analysis allowed further separation of a batch of tourmaline-rich samples with a B_2O_3 content >1%, corresponding to tourmalinites with >15 vol% tourmaline (as defined by Slack *et al.*, 1984). Estimate of the tourmaline content of rocks was made by knowing the rock B concentration determined by GF-AAS, by considering the average concentration of B_2O_3 in the analyzed tourmalines and by assuming that all B is included in tourmaline, as the only B-bearing phase present.

Tourmaline Chemistry

Tourmaline compositions may be represented by the general formula $X\,Y_3\,Z_6\,(BO_3)_3\,T_6\,O_{18}\,V_3\,W$, for which X = Na, Ca, K, vacancies; Y = Mg, Fe^{2+}, Fe^{3+}, Li, Al, Mn, Ti^{4+}, Cr^{3+}; Z = Al, Mg, Fe^{3+}, Cr^{3+}; T = Si, Al; V = OH, O; W = OH, F, O (Hawthorne and Henry, 1999). Cation contents have been calculated from the electron microprobe data on the basis of 31 oxygen atoms with 3 B and 4

TABLE 1

Representative electron microprobe analyses of the four types of tourmaline in the Val Trompia tourmalinites. Average composition and corresponding standard deviation for tourmaline crystals from the pegmatite dike associated with the granitoid intrusion at Maniva Pass is included for comparison.

	Type I				Type II				Type III			Type IV							Maniva Pass	
	430	450	410	32	469	479	48	49	34	37	38	880/10	880/5	880/7	vn23/7	vn23/8	vm8/4	vm8/1	n=15	
SiO_2	36.63	36.38	36.48	37.04	36.98	37.31	36.93	37.24	37.70	36.35	37.97	34.23	33.28	33.24	36.54	36.22	36.36	35.02	36.69	(0.71)
TiO_2	0.72	0.61	0.74	0.63	0.45	0.23	0.31	0.16	0.42	1.97	0.65	0.40	0.39	0.31	0.31	0.61	0.33	0.45	0.73	(0.13)
Al_2O_3	30.93	31.06	31.34	31.91	32.45	35.32	35.36	34.76	27.16	27.47	29.04	24.09	18.91	18.27	23.46	23.72	28.60	28.98	31.40	(0.49)
FeO	8.22	8.87	7.97	8.13	5.63	3.62	3.73	4.61	13.50	12.70	11.66	22.46	30.83	31.14	22.91	21.48	17.70	17.32	8.83	(0.51)
MnO	0.03	0.05	0.03	0.04	0.03	0.00	0.03	0.00	0.01	0.02	0.05	0.04	0.02	0.04	0.05	0.05	0.00	0.02	0.02	(0.02)
MgO	7.02	6.88	7.42	7.29	7.84	7.94	8.35	8.14	5.77	5.43	4.95	2.79	1.49	1.23	2.75	2.77	3.29	3.01	6.77	(0.32)
CaO	0.77	0.79	1.00	0.82	0.75	0.63	0.84	0.42	0.63	0.71	0.59	0.42	0.24	0.18	0.62	0.60	0.41	0.48	0.60	(0.13)
Na_2O	2.30	2.19	1.95	1.91	2.51	2.54	2.44	2.47	2.57	2.37	2.33	2.49	2.64	2.59	2.39	2.60	2.67	2.34	2.20	(0.12)
K_2O	0.03	0.01	0.01	0.01	0.03	0.01	0.01	0.01	0.03	0.03	0.02	0.05	0.12	0.14	0.05	0.05	0.05	0.03	0.04	(0.01)
B_2O_3§	10.60	10.59	10.66	10.77	10.76	11.02	11.05	10.99	10.44	10.36	10.52	9.76	9.33	9.23	10.03	9.98	10.39	10.20	10.66	
total	97.25	97.43	97.60	98.55	97.43	98.63	99.05	98.81	98.23	97.41	97.78	96.73	97.25	96.36	99.11	98.08	99.80	97.85	97.94	
B	3.000	3.000	3.000	3.000	3.000	3.000	3.000	3.000	3.000	3.000	3.000	3.000	3.000	3.000	3.000	3.000	3.000	3.000	3.000	
Si	6.005	5.971	5.951	5.975	5.973	5.882	5.811	5.886	6.278	6.099	6.272	6.099	6.202	6.269	6.334	6.310	6.078	5.970	5.809	(0.067)
Al_T	0.000	0.029	0.050	0.025	0.027	0.119	0.189	0.114	0.000	0.000	0.000	0.000	0.000	0.000	0.000	0.000	0.000	0.030	0.191	
Al_Z	6.000	6.000	6.000	6.000	6.000	6.000	6.000	6.000	5.330	5.432	5.653	5.058	4.152	4.061	4.792	4.871	5.636	5.791	6.000	(0.000)
Al_Y	0.000	0.000	0.000	0.042	0.151	0.444	0.369	0.361	0.000	0.000	0.000	0.000	0.000	0.000	0.000	0.000	0.000	0.000	0.423	
Ti	0.089	0.076	0.091	0.077	0.055	0.028	0.037	0.019	0.053	0.249	0.081	0.054	0.055	0.043	0.041	0.080	0.042	0.057	0.077	(0.015)
Fe	1.127	1.218	1.087	1.097	0.761	0.477	0.491	0.610	1.880	1.782	1.611	3.346	4.805	4.910	3.320	3.130	2.475	2.469	1.088	(0.066)
Mn	0.004	0.007	0.004	0.006	0.004	0.000	0.004	0.000	0.002	0.003	0.007	0.050	0.003	0.007	0.008	0.007	0.000	0.003	0.008	(0.004)
Mg	1.716	1.684	1.805	1.753	1.888	1.866	1.959	1.918	1.433	1.358	1.219	0.740	0.413	0.344	0.711	0.721	0.820	0.764	1.290	(0.080)
Ca	0.135	0.139	0.175	0.142	0.130	0.107	0.142	0.071	0.113	0.128	0.105	0.080	0.049	0.037	0.115	0.112	0.073	0.088	0.109	(0.023)
Na	0.731	0.697	0.617	0.598	0.786	0.777	0.745	0.757	0.830	0.771	0.746	0.860	0.954	0.945	0.805	0.878	0.866	0.774	0.610	(0.037)
K	0.007	0.002	0.002	0.002	0.006	0.002	0.002	0.002	0.007	0.007	0.004	0.011	0.029	0.033	0.012	0.011	0.010	0.006	0.006	(0.003)
XTotal	0.873	0.838	0.794	0.741	0.922	0.885	0.888	0.830	0.949	0.905	0.855	0.950	1.031	1.015	0.932	1.002	0.949	0.868	0.725	
Mg/Fe	1.52	1.38	1.66	1.60	2.48	3.91	3.99	3.14	0.85	0.77	0.76	0.22	0.09	0.07	0.21	0.23	0.33	0.31	1.19	

n = number of analyses; numbers in parentheses are standard deviations of the mean; B_2O_3§ is calculated on the basis of 3 apfu

(OH) assumed so that the factor used is 24.5 oxygen atoms. An approach equal to that of other Authors (e.g. Foit and Rosenberg, 1977; Gallagher, 1988) was followed in the site filling. B_2O_3 is calculated on the assumption of stoichiometric 3 B atoms per formula unit (a.p.f.u.). Six Al atoms are placed in the Z site; Si is exclusively in the tetrahedral site. If calculated Si is less than 6, Al is used to fill the tetrahedral site (Foit and Rosenberg, 1977) even if Al does not exceed 6 atoms. Any remaining Al not assigned in the previous sites is placed in the Y site.

Val Trompia tourmalines

Representative analyses of the Val Trompia tourmalines are given in Table 1, where four types are distinguished based on textures and compositions. Table 1 also includes the average value and corresponding standard deviation for tourmaline crystals from a pegmatite associated with the granitoid intrusion at Maniva Pass.

Compositions of most analyzed points may be generally ascribed to the schorl-dravite solid solution series. Principal variations involve Fe and Mg for type I and II tourmalines but Fe and Al, and to a lesser extent Mg, vary for type III and IV tourmalines. Tourmalines of different types and compositions may occur in the same sample. Mg/Fe ratios clearly discriminate the four tourmaline types. Type I tourmalines are characterized by Mg/Fe from 1.38 to 1.66; type II by Mg/Fe from 2.48 to 3.99; type III tourmalines by Mg/Fe of about 0.7 and the type IV by Mg/Fe less than 0.35. An extraordinary abundance of Fe is shown by type IV tourmaline, that forms rims on the µm-sized acicular crystals bordering the youngest quartz-tourmaline veinlets. In these rims the Mg/Fe ratio can be as low as 0.01. By BSE imaging, the Fe-rich rims are sharply distinguished from the cores, which show an irregular morphology (like fragments) and a composition comparable with that of type III tourmaline (fig. 3*d*).

According to the newest classification of Hawthorne and Henry (1999), the Val Trompia tourmalines plot within the field of «alkali group» varieties (fig. 6*a*), with Na+K dominant in the X site and a moderate tendency to X-site vacancies. Data about occupancy of the OH-bearing sites (V and W), necessary for this new classification scheme, are however incomplete, as only F was analyzed and is below detection limits. Therefore it is assumed that OH occupies the W site in type I and II tourmalines, with Y site dominated by bivalent cations. Assumption of the V site occupancy by OH is based on current knowledge (*in* Hawthorne and Henry, 1999). The Z site is totally occupied by Al in type I and II tourmalines, whereas it is moderately to highly deficient in Al (4.06 a.p.f.u.) in type III and IV tourmalines.

As shown in figure 7*a*, the Y site is occupied by Mg, Fe, and Al (the presence of Li is excluded): most data points are along the schorl-dravite solid solution line. However, several points (corresponding to type III and IV compositions) project towards the $FeAl_{-1}$ (povondraite) substitution. High Fe values linked to an excess of cations in the Y site and an inverse correlation between Fe and Al shown in figure 7*b*, may suggest some Fe substitution for Al in the Z site, thereby requiring the presence of both ferrous and ferric iron (Henry and Guidotti, 1985; London and Manning, 1995; Fuchs *et al.*, 1998). An approximate evaluation of contents in Fe^{3+} (typical of the povondraite component) according to the method by Lynch and Ortega (1997), would indicate Fe^{3+} variable between 0.012 and 2.217 a.p.f.u. in type III and type IV tourmalines. In some crystals, estimated Fe^{3+} is not sufficient to fill the vacancy in the Z site, thereby requiring the presence of other cations (e.g., Mg^{2+}; *in* Hawthorne *et al.*, 1993). Mössbauer spectroscopy measurements and X ray refinements would however be necessary to assess the actual mode of occupancy in the Z site of type III and IV tourmalines. Also higher K contents in type IV tourmalines are compatible with the possible presence of povondraite component, even if the Mg contents are lower than the theoretical ideal (Grice *et al.*, 1993). In case of presence of Fe^{3+},

TABLE 2

Electron microprobe analyses of the coarse tourmaline
Average compositions and related standard deviations are indicated. Data for a tourmaline crystal

	C17	T1B	T2	T3A	T5A	T7	T100B
	n=19	n=11	n=3	n=11	n=11	n=5	n=5
SiO_2	37.22 *0.50*	37.21 *0.31*	37.18 *0.34*	35.42 *0.99*	37.11 *0.36*	37.17 *0.28*	36.72 *0.30*
TiO_2	0.51 *0.28*	0.80 *0.08*	0.82 *0.06*	0.78 *0.49*	0.63 *0.25*	1.02 *0.29*	0.80 *0.17*
Al_2O_3	32.43 *2.63*	32.24 *1.00*	30.71 *0.33*	29.71 *0.65*	31.37 *2.34*	31.73 *1.13*	32.35 *1.72*
FeO	9.00 *3.30*	7.63 *1.34*	5.50 *0.33*	11.64 *1.36*	9.57 *2.71*	7.87 *1.61*	8.03 *1.08*
MnO	0.03 *0.02*	0.01 *0.01*	0.02 *0.02*	0.03 *0.02*	0.02 *0.02*	0.03 *0.03*	0.01 *0.01*
MgO	6.15 *0.63*	7.31 *0.55*	9.18 *0.20*	5.76 *0.63*	6.86 *0.92*	7.43 *0.51*	6.60 *0.45*
CaO	0.53 *0.31*	0.38 *0.11*	0.44 *0.01*	0.48 *0.29*	0.57 *0.51*	0.36 *0.24*	0.39 *0.12*
Na_2O	2.18 *0.31*	2.39 *0.20*	2.60 *0.08*	2.38 *0.22*	2.23 *0.24*	2.55 *0.24*	2.16 *0.37*
K_2O	0.02 *0.02*	0.02 *0.01*	0.05 *0.01*	0.12 *0.12*	0.03 *0.01*	0.02 *0.01*	0.03 *0.02*
B_2O_3§	10.78	10.83	10.73	10.34	10.76	10.82	10.71
total	98.85	98.82	97.23	96.66	99.15	99.00	97.80
B	3.000	3.000	3.000	3.000	3.000	3.000	3.000
Si	6.002 *0.065*	5.972 *0.026*	6.025 *0.015*	5.952 *0.136*	5.995 *0.056*	5.971 *0.045*	5.962 *0.042*
Al_T	0.000	0.028	0.000	0.048	0.005	0.029	0.038
Al_Z	6.000 *0.295*	6.000 *0.048*	5.864 *0.046*	5.909 *0.096*	6.000 *0.294*	5.980 *0.073*	6.000 *0.049*
Al_Y	0.153	0.071	0.000	0.000	0.084	0.000	0.148
Ti	0.062 *0.036*	0.096 *0.009*	0.100 *0.007*	0.099 *0.063*	0.077 *0.029*	0.124 *0.036*	0.097 *0.022*
Fe	1.222 *0.489*	1.026 *0.185*	0.745 *0.041*	1.637 *0.204*	1.295 *0.383*	1.058 *0.223*	1.092 *0.159*
Mn	0.004 *0.003*	0.001 *0.002*	0.002 *0.003*	0.005 *0.003*	0.003 *0.002*	0.004 *0.004*	0.002 *0.002*
Mg	1.477 *0.137*	1.748 *0.118*	2.217 *0.026*	1.442 *0.145*	1.652 *0.222*	1.778 *0.113*	1.598 *0.121*
Ca	0.091 *0.052*	0.066 *0.018*	0.077 *0.002*	0.087 *0.053*	0.099 *0.091*	0.061 *0.040*	0.067 *0.019*
Na	0.683 *0.113*	0.743 *0.064*	0.815 *0.017*	0.774 *0.065*	0.699 *0.077*	0.794 *0.080*	0.681 *0.126*
K	0.005 *0.005*	0.005 *0.001*	0.010 *0.001*	0.026 *0.027*	0.007 *0.003*	0.005 *0.002*	0.006 *0.005*
XTotal	0.779	0.814	0.902	0.887	0.805	0.860	0.754
Mg/Fe	1.21	1.70	2.98	0.88	1.28	1.68	1.46

n = number of analyses; * data from Slack (1996); in italics are standard deviations of the mean; B_2O_3§ is

crystals in the Orobic tourmalinites at Lake Diavolo.
from the inner alteration zone at Novazza (Slack, 1996) are also included for comparison.

T100C	**T101**	**T102A**	**T102B**	**T103**	**T104**	**T106**	**T107**	**Nov ***
n=4	n=11	n=2	n=6	n=2	n=1	n=8	n=5	n=1
36.52 *0.34*	37.17 *0.36*	37.56 *0.15*	34.85 *0.36*	36.28 *0.16*	36.07	37.38 *0.31*	36.56 *0.34*	36.27
0.83 *0.11*	0.52 *0.19*	0.76 *0.05*	0.06 *0.02*	0.93 *0.01*	0.75	0.74 *0.21*	1.07 *0.63*	0.07
32.02 *1.38*	33.39 *0.41*	33.93 *0.03*	24.14 *0.75*	30.54 *0.00*	32.02	32.78 *1.04*	31.65 *1.39*	36.88
8.78 *1.85*	7.14 *0.94*	7.08 *0.47*	17.91 *2.02*	8.67 *0.28*	7.90	8.62 *0.66*	7.13 *2.45*	11.08
0.01 *0.01*	0.01 *0.01*	0.00 *0.00*	0.01 *0.01*	0.01 *0.01*	0.01	0.02 *0.01*	0.01 *0.01*	0.00
6.24 *0.66*	6.64 *0.99*	6.76 *0.10*	5.46 *0.59*	6.71 *0.01*	6.52	6.42 *0.50*	7.52 *1.27*	2.34
0.41 *0.18*	0.66 *0.18*	0.37 *0.01*	2.26 *0.39*	0.55 *0.01*	0.43	0.36 *0.15*	0.83 *0.34*	0.02
2.24 *0.27*	1.92 *0.16*	2.05 *0.02*	1.58 *0.20*	2.34 *0.02*	2.07	2.20 *0.42*	2.04 *0.30*	0.76
0.03 *0.00*	0.02 *0.01*	0.03 *0.01*	0.04 *0.00*	0.03 *0.01*	0.07	0.02 *0.00*	0.03 *0.02*	0.60
10.65	10.83	10.97	9.90	10.50	10.55	10.86	10.69	
97.73	98.30	99.51	96.21	96.56	96.39	99.40	97.53	87.48
3.000	3.000	3.000	3.000	3.000	3.000	3.000	3.000	3.000
5.959 *0.044*	5.968 *0.037*	5.951 *0.004*	6.118 *0.048*	6.002 *0.001*	5.942	5.980 *0.028*	5.942 *0.043*	5.870
0.041	0.032	0.050	0.000	0.000	0.058	0.020	0.058	0.130
6.000 *0.000*	6.000 *0.000*	6.000 *0.000*	4.995 *0.153*	5.956 *0.025*	6.000	6.000 *0.000*	6.000 *0.132*	6.000
0.115	0.286	0.287	0.000	0.000	0.159	0.160	0.003	0.904
0.102 *0.015*	0.063 *0.023*	0.090 *0.006*	0.007 *0.003*	0.116 *0.002*	0.093	0.089 *0.025*	0.132 *0.100*	0.009
1.200 *0.265*	0.960 *0.131*	0.938 *0.059*	2.629 *0.297*	1.200 *0.035*	1.089	1.153 *0.091*	0.974 *0.366*	1.500
0.001 *0.001*	0.001 *0.001*	0.000 *0.000*	0.002 *0.002*	0.001 *0.002*	0.001	0.002 *0.001*	0.001 *0.002*	0.000
1.515 *0.143*	1.587 *0.228*	1.597 *0.028*	1.428 *0.151*	1.655 *0.004*	1.600	1.532 *0.118*	1.818 *0.320*	0.564
0.070 *0.030*	0.113 *0.031*	0.063 *0.003*	0.426 *0.074*	0.096 *0.002*	0.077	0.062 *0.026*	0.145 *0.077*	0.003
0.711 *0.095*	0.597 *0.047*	0.629 *0.010*	0.538 *0.068*	0.750 *0.004*	0.661	0.681 *0.136*	0.645 *0.121*	0.238
0.006 *0.001*	0.004 *0.002*	0.005 *0.001*	0.009 *0.001*	0.006 *0.001*	0.015	0.005 *0.001*	0.005 *0.003*	0.012
0.787	0.713	0.697	0.972	0.852	0.752	0.748	0.794	0.253
1.26	1.65	1.70	0.72	1.38	1.47	1.33	1.87	0.38

calculated on the basis of 3 apfu

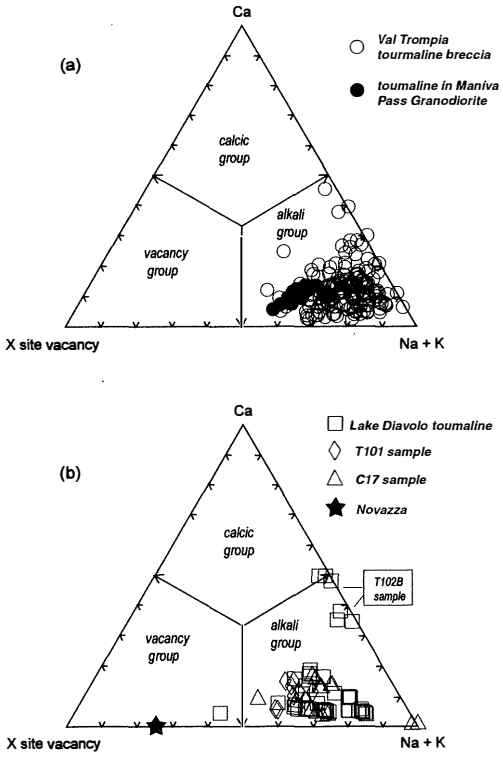

Fig. 6 – Composition of Val Trompia *(a)* and Lake Diavolo *(b)* tourmalines on the basis of the X-site occupancy (after Hawthorne and Henry, 1999).

type III and IV tourmaline might have O^{2-} in the W site (Grice and Ercit, 1993).

The Al-Fe-Mg ternary diagram (Henry and Guidotti, 1985) in fig. 8*a* allows tourmaline compositions to be compared to those of the parental rocks and highlights distinct compositional trends for types I, II, and III relative to type IV tourmalines. The first three types mostly occupy fields 4 and 5, and partly field 6 at the limit with field 3. Such compositions are variably constrained by the chemistry of the precursor (untourmalinized) metamorphic rock (phyllite), and tend slightly towards compositions showing an affinity with granites (field 3). The sharply discordant trend of type IV tourmalines is parallel to the Fe-Al axis and crosses the line $Al_{50}Fe_{50}$-$Al_{50}Mg_{50}$, considered by Henry and Guidotti, (1985) as an extreme boundary. This trend lies completely within field 3 and is characteristic of high Fe^{3+} tourmalines (Cavarretta and Puxeddu, 1990), and those related to the hydrothermal alteration of granites.

Lake Diavolo Tourmalines

Table 2 shows average compositions and related standard deviations for 64 analytical points corresponding to the coarse tourmaline grains (maximum size 50 μm) isolated in the cryptocrystalline groundmass of the contact-zone tourmalinites, and to tourmaline crystals in metamorphic (C17) and quartz vein clasts (T101) in the conglomerates. Data relative to a tourmaline crystal from the inner alteration

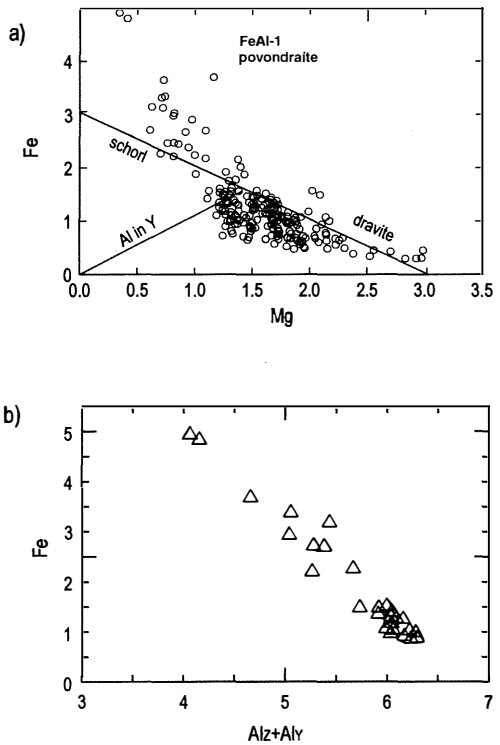

Fig. 7 – *(a)* Fe *vs* Mg (a.p.f.u.) for all analyses of the Val Trompia tourmalines. *(b)* Al^{VI} *vs* Fe (a.p.f.u.) for type III and IV tourmalines from the Val Trompia samples.

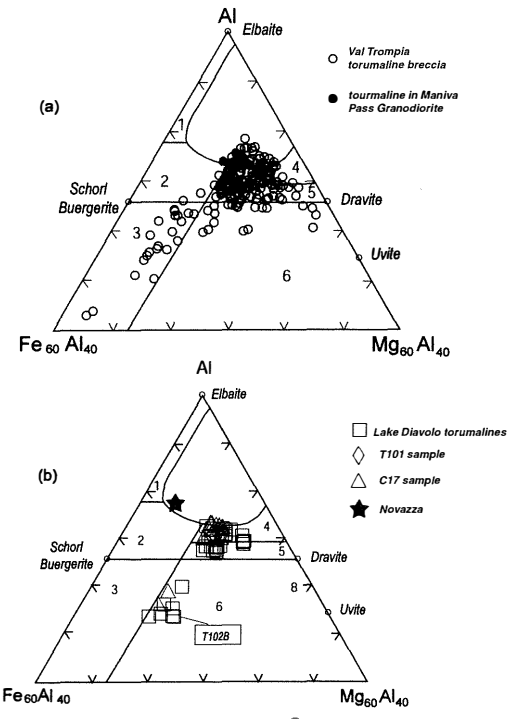

Fig. 8 – Al-Fe-Mg relationships for the Val Trompia *(a)* and Lake Diavolo *(b)* tourmalines. Field numbers as in Henry and Guidotti (1985). Any tourmaline plotting below the schorl(buergerite)-dravite join will have Al < 6 a.p.f.u..

zone at the Novazza U deposit (from Slack, 1996) are also included for comparison.

The overall composition of the coarse tourmaline grains is comparable to that of the type I and II tourmalines from Val Trompia (fig. 6*b* and fig. 8*b*). Tourmaline crystals in the quartz vein fragment in conglomerate (sample T101) are fully consistent with the main composition. The only samples that deviate from the general trend are T102B and, partially, C17. Sample T102B contains to a relic blue-green tourmaline relatively enriched in Ca (>0.4 a.p.f.u.) and Fe (2.629 a.p.f.u.). Sample C17 has tourmaline crystals with a heterogeneous composition showing major variations in Fe and Al. On the whole Si approximates to 6 a.p.f.u., with the Z site nearly full except in sample T102B. The Y site is almost fully occupied by Fe, Mg (slightly variable amounts) and Al.

According to Hawthorne and Henry's (1999) new classification, the coarse Orobic tourmalines are generally defined as alkali group varieties, with the sum of the X-site cations ranging between 0.697 to 0.972 a.p.f.u. (fig. 6*b*). The higher values correspond to more calcic compositions relative to sample T102B.

In fig. 8*b*, most data points plot along and above the schorl-dravite join, with the exception of samples T102B and partly C17 (tourmaline-bearing metamorphic fragment in conglomerate) due to their relatively Al-poor, Fe-rich nature. The majority of the coarse-grained tourmalines in the metasomatized cataclasites and the coarse tourmaline crystals associated with undeformed vein quartz found in conglomerate (sample T101) occupy fields 4 and 5, similar to the type I and main-stage type II Val Trompia tourmalines, and correspond to compositions with affinities to the basement phyllites. This may be dependent on the contribution of components for the crystallization of the metasomatic tourmalines by the basement-derived phyllosilicate-rich matrix of the Permian terrigenous rocks involved in the cataclasis along the contact-zone.

In figs 6*b* and 8*b* the Novazza inner-zone tourmaline differs from the coarse Orobic tourmalines in displaying an evident alkali defect and a more schorlitic composition with Al_Y enrichment. At Novazza compositions comparable with the Orobic coarse tourmalines are exhibited by the external zone tourmalines (in Fuchs and Maury, 1995).

Whole-rock Compositions of Tourmalinites

Table 3*a-b* includes whole-rock analyses for major, minor, and some trace elements in the Val Trompia and Lake Diavolo tourmalinites. Tourmalinite samples from Val Trompia derive from the larger outcrops near Graticelle, Roccolo Pomo and Memmo, and were selected based on textural variations and different degrees of fracture-related tourmalinization.

TABLE 3

a) - Whole-rock compositions of selected tourmaline breccia samples from Val Trompia; b) - Whole-rock compositions of tourmalinites from Lake Diavolo. Major and minor elements are in weight %, trace elements in ppm.

a)	*RDC-1* *a*	*RDC-2* *b*	*RDC-3A* *c*	*RDC-3B* *d*	*RDC-4* *e*	*RDC-7* *f*	*RDC-8* *g*	*RDC-11A* *h*	*RDC-13* *i*
SiO_2	72.77	79.18	61.12	54.86	72.39	75.39	58.63	64.88	72.39
TiO_2	0.95	0.52	0.76	1.19	0.67	1.26	0.88	0.81	0.62
Al_2O_3	12.51	10.90	12.48	15.52	11.41	14.08	13.40	15.05	14.28
FeO	2.65	2.16	3.62	3.57	3.33	1.87	4.25	2.77	1.73
Fe_2O_3	4.82	2.96	7.32	5.03	4.52	2.33	6.60	4.00	1.65
MnO	0.14	0.02	0.06	0.01	0.07	0.01	0.02	0.02	0.02
MgO	1.04	0.94	3.71	8.21	1.41	1.06	4.65	2.43	0.90
CaO	0.32	0.20	0.32	0.77	0.21	0.27	0.40	0.34	0.29
Na_2O	1.03	1.03	1.29	1.10	1.05	1.05	1.36	4.11	4.68
K_2O	0.06	0.05	0.10	0.15	0.14	0.03	0.03	0.11	0.73
P_2O_5	0.19	0.05	0.07	0.08	0.06	0.05	0.05	0.10	0.13
LOI	1.82	1.33	2.45	3.17	2.06	0.84	2.22	1.88	1.04
Ba	142	20	67	10	48	20	15	50	113
Rb	<5	<5	<5	<5	<5	<5	<5	<5	20
Sr	130	97	201	225	140	95	219	123	75
Y	31	15	25	18	35	31	23	40	15
Nb	17	7	6	10	8	27	15	13	11
Zr	273	132	130	192	245	263	162	193	360
Sc	11	7	19	24	9	9	16	12	6
Cr	66	41	54	66	44	85	62	52	36
V	96	82	112	177	105	142	133	95	85
Co	23	14	37	23	28	12	37	23	8
Ni	22	19	55	259	24	34	84	43	13
Zn	9	5	26	20	15	5	18	<5	38
Pb	6	8	10	11	6	8	10	7	13
Th	8	<5	7	<5	<5	12	<5	8	10
La	97.03	8.89			49.21			40.44	20.48
Ce	199.8	18.39			96.19			93.81	35.58
Pr	22.26	1.95			10.46			11.04	3.41
Nd	80.03	7.30			40.57			44.16	12.37
Sm	14.08	1.30			6.65			9.49	1.95
Eu	2.94	0.35			1.20			2.57	0.39
Gd	8.12	0.94			4.48			7.19	1.87
Tb	1.00	0.19			0.62			1.14	0.32
Dy	5.41	1.31			4.46			7.01	1.98
Ho	1.19	0.43			1.28			1.56	0.46
Er	3.92	1.51			3.77			4.13	1.20
Tm	0.71	0.3			0.62			0.64	0.20
Yb	4.61	2.09			3.94			4.13	1.34
Lu	0.74	0.33			0.50			0.64	0.20
$(La/Yb)_N$	14.07	2.84			8.35			6.55	10.22
Eu/Eu*	0.84	0.97			0.68			0.96	0.63

TABLE 3, *continued*

b)	*T3A*	*T7*	*T100C*	*T100B*	*T102A*	*T102B*	*T103*	*T104*	*T106*	*T107*
SiO_2	54.49	57.59	63.50	63.69	67.28	68.60	72.12	77.44	67.81	71.42
TiO_2	1.11	1.01	0.79	0.81	0.54	0.50	0.39	0.17	0.51	0.40
Al_2O_3	18.67	18.35	16.43	16.56	15.15	15.48	11.88	10.95	14.09	12.67
Fe_2O_3 t	9.57	8.00	6.84	6.74	5.41	4.51	6.86	4.25	7.49	6.09
MnO	0.02	0.02	0.01	0.01	0.01	0.01	0.01	0.02	0.05	0.01
MgO	2.75	3.27	2.17	2.30	1.45	1.72	1.44	0.46	1.68	1.03
CaO	0.07	0.16	0.05	0.08	0.20	0.05	0.04	0.02	0.00	0.03
Na_2O	1.11	1.14	1.18	1.22	1.19	0.61	0.96	0.48	0.86	0.79
K_2O	3.70	1.60	2.35	2.57	2.68	3.63	0.86	2.35	2.04	1.51
P_2O_5	0.10	0.12	0.06	0.08	0.08	0.07	0.06	0.03	0.07	0.06
B_2O_3	4.16	5.12	3.97	3.81	3.21	1.69	3.86	2.41	3.27	3.22
LOI	4.05	3.56	3.18	3.08	2.59	2.89	2.39	1.88	3.11	2.49
Ba	161	158	147	151	264	320	104	112	144	150
Rb	235	109	141	156	153	191	54	99	101	74
Sr	220	362	159	155	127	104	267	110	147	148
Y	21	21	22	21	22	22	25	25	22	24
Nb	25	19	20	20	16	14	6	10	11	16
Zr	262	233	190	193	168	156	132	117	124	158
Sc	19	10	10	12	9	7	8	9	11	9
Cr	66	65	42	44	33	32	28	9	41	22
V	135	136	102	100	71	70	44	19	66	52
Co	25	25	21	22	11	9	17	9	22	11
Ni	50	95	56	58	25	18	11	5	17	10
Zn	99	115	84	68	49	43	108	78	46	65
Pb	36	24	12	22	14	23	10	14	21	7
Th	174	71	25	109	9	55	<5	<5	19	<5

a) breccia with metamorphic quartz clasts and minor late quartz veining;
b) breccia with metamorphic quartz clasts and minor late quartz veining;
c) tourmaline-rich breccia with phyllite fragments;
d) black, massive, fine-grained tourmalinite with rare quartz fragments;
e) tourmaline breccia rich in metamorphic polycrystalline quartz fragments;
f) breccia with highly strained quartz matrix; tourmaline crystallization along foliation planes;
g) breccia moderately tourmalinized along cataclastic zones;
h) paragneiss breccia rich in tourmaline grown in highly strained quartz matrix;
i) paragneiss breccia; tourmalinization along foliation plans; presence of albite and sericite.

The analyzed Lake Diavolo samples correspond to the most tourmaline-rich rocks distinguished on the basis of their high B_2O_3 contents (measured by GF-AAS); these samples contain coarse tourmaline crystals that were analyzed by microprobe.

Whole-rock data for the Val Trompia tourmalinites show wide variations in major

and minor element concentrations. These variations mainly reflect the relative proportion of tourmaline versus vein quartz and/or relic fragments of host schists. Tourmaline is however the main mineral component, exceeding 70% volume of total rock. Trace element contents lack any systematic internal variations.

Whole-rock data for the Lake Diavolo tourmalinites are comparable with data presented by Slack *et al.* (1996) for the sampling sites indicated in fig. 4. Fluctuations in element concentrations are presumably dependent on the fraction of lithic components present in the metasomatized cataclasites, relative to tourmaline abundance.

Differences between the Val Trompia and Lake Diavolo tourmalinites are highlighted by some trace element contents. The large ion lithophile elements (LILE) are more enriched in the Lake Diavolo samples, together with Th, Zn and Pb. Slack *et al.* (1996) also reported the presence of high Be in the tourmalinites from the Lake Diavolo and Lake Publino areas, which they considered strongly suggestive of a magmatic component in the tourmalinizing fluids.

Val Trompia tourmalinites show relative enrichment in immobile elements (Zr, Y and Sc) and depletion in mobile elements (Rb, Ba, Zn and Sr), if compared with the compositions of Lake Diavolo tourmalinites. This may be related to stronger mass loss in the metasomatized protolith at Val Trompia, with consequent remobilization of mobile elements during tourmalinization, as observed by Slack *et al.* (1996). The intensity of tourmalinization at Val Trompia was presumably stronger than at Lake Diavolo. Local Ni enrichments in Val Trompia samples may be due to the presence of accessory sulphides (mainly pyrite).

Chondrite-normalized REE data for the Val Trompia tourmalinites are presented in fig. 9, where profiles for Torgola granite (De Capitani *et al.*, 1994) and basement schists and Orobic tourmalinites (Slack *et al.*, 1996) are shown for comparison. REE profiles for all Val Trompia samples are characterized by steep LREE trends and moderate to high LREE contents or slightly negative Eu anomalies, and a tendency towards slight HREE enrichment. The observed REE profiles may be attributed to effects of hydrothermal fluids, and not necessarily to the nature of the metasomatized protolith. Relative enrichments in LREE are compatible with mechanisms of transport and preferential deposition of LREE from hydrothermal fluids, in which LREE-bearing complexes are less stable than HREE-bearing ones (Taylor and Fryer, 1982). The weak or absent Eu anomaly may also be explained as relative Eu enrichment related to the hydrothermal fluids (MacLean, 1988). The shape of the REE pattern resembles profiles typical of tourmaline (Alderton, *et al.*, 1980; King *et al.*, 1988). The trends of whole-rock LREE enrichment are confirmed by similar enrichments in tourmaline crystals belonging to the main stage of tourmalinization (type II tourmalines), as shown by preliminary ion probe analyses (Grieco *et al.*, in preparation). This suggests that LREE enrichments in the Val Trompia tourmalinites may be ascribed primarily to tourmaline crystallization and not to precipitation of LREE-rich accessory minerals (e.g., monazite, allanite).

The REE field of the Orobic tourmalinites, reported in fig. 9, differs from the Val Trompia trend in having negative Eu anomalies and generally lower La/Yb ratios, similar to the REE profiles obtained by Slack *et al.* (1996) for the unaltered (and tourmaline-free) conglomerate and sandstone host rocks in the Lake Diavolo and Lake Publino areas.

DISCUSSION

Geological, textural, and geochemical data presented here for the Val Trompia tourmalinites allow assessment of the metasomatic nature of these rocks and reconstruction of a model for their formation. The Val Trompia tourmalinites exhibit textural and mineralogical features comparable with

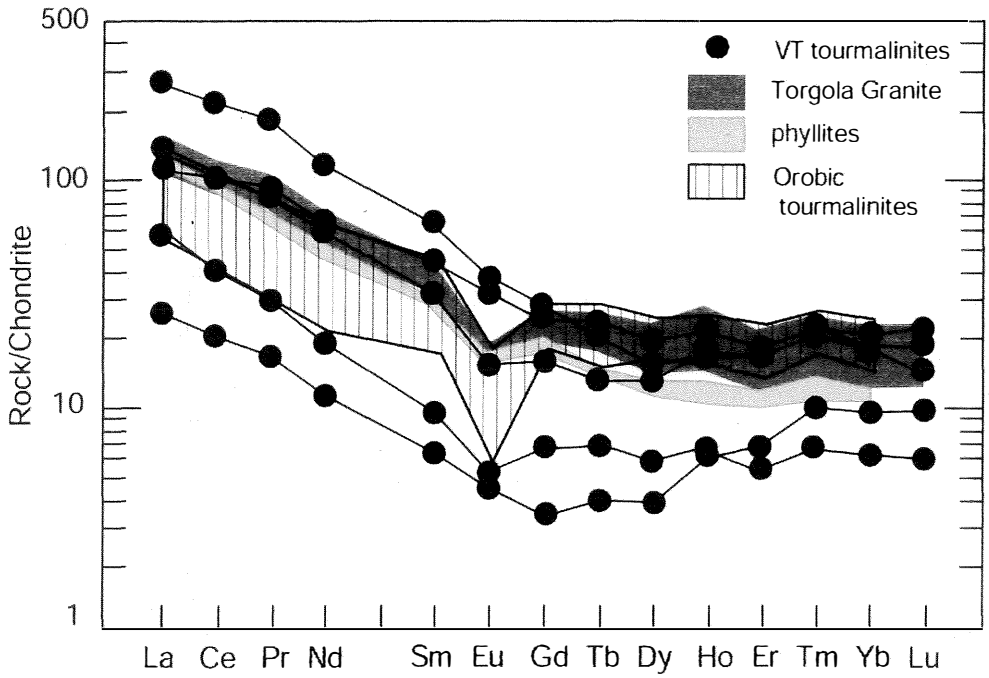

Fig. 9 – Chondrite-normalized REE patterns for selected Val Trompia tourmaline breccias. REE profiles from the Torgola granite (De Capitani *et al.*, 1994), and from phyllites and the Orobic tourmalinites (Slack *et al.*, 1996) are reported for comparison. Chondrite data from Nakamura (1974).

those of hydrothermal tourmaline-rich breccias in apical parts of the Variscan granites of Cornwall, England (Allman-Ward *et al.*, 1982; London and Manning, 1995). Like the Cornish tourmalinites, the Val Trompia tourmalinites show hydraulic breccia textures that have been interpreted to result from explosive release (decompression) of B-rich, saline magmatic fluids from the apical parts of the granite, accompanied by hydrofracturing and boron metasomatism of the host rocks (Allman-Ward *et al.*, 1982).

The Val Trompia tourmalinites are geologically related to a well-defined geological-structural framework, which includes late-post-orogenic, shallow K-Al-rich granitic rocks of upper Palaeozoic age emplaced along regional crustal fractures, and systems of hydrothermal veins containing Sn-W and base-metal mineralization. A direct correlation between host-rock tourmalinization and the Torgola granite intrusion cannot be proved sofar. A suggestion may however come from the recognized effect of B in greatly lowering solidus temperatures in granitic melts (Pollard *et al.*, 1987; Dingwell *et al.*, 1996, and references therein). Boron enrichment in the Torgola magma would justify the low temperatures of crystallization (below 600°C) recorded by De Capitani *et al.* (1994). The limited exposures of the Torgola complex do not show any evidence of tourmaline. However, they may not necessarily correspond to the apical parts of the pluton, that may have been eroded away during Upper Permian time.

Tourmalinization occurred in a succession of distinct stages of brecciation and metasomatism of the host rock. A time-related sequence of crystallization is recognizable, recording rapid changes in the chemistry of the metasomatic

fluid. The main tourmalinizing event (type II schorl-dravite tourmalines) was strongly influenced by the composition of the host basement schists. Only the later generations of tourmaline show an affinity with fluids having a magmatic source, evidenced mainly through a progressive increase in Fe. The enrichment in Fe^{3+} in type III and IV, if confirmed by Mössbauer analyses, and the consequent crystallization of povondraite-type tourmalines in late veinlets may indicate a sudden change in the fluid oxidation state. Coupled substitution of Fe-Al and dramatic increases of Fe^{3+} with oxidation of the magmatic-hydrothermal fluid may be interpreted to reflect progressive influx of meteoric water to the hydrothermal system with increasing distance from the granite contact, as observed in the Larderello geothermal field in Tuscany, Italy, and in the Sn-W province of Cornwall, southwest England (Cavarretta and Puxeddu, 1990; London and Manning, 1995). Saline, highly oxidized fluids are also compatible with magmatic-hydrothermal systems like porphyry Cu deposits, which are locally enriched in tourmaline (e.g., Slack, 1996; Lynch and Ortega, 1997). The transition from an «internal» magmatic-hydrothermal system, to an «external» one, dominated by meteoric fluids, is characterized by drastic changes in T, P, pH, salinity, and styles of alteration and/or mineralization (Cavarretta and Puxeddu, 1990; Fuchs and Maury, 1995). In Val Trompia similar changes in hydrothermal conditions may be indicated by relative positions of the tourmalinite samples containing povondraite (fig. 10). To the east, late faulting brought the pluton closer to the surface and erosion removed the apical parts of the magmatic-hydrothermal system. There, only the deeper parts of the alteration system closest to the pluton (main stage tourmalinization) are preserved. To the west of the samples with Fe-rich tourmalines is the area marking the «external» zone of the system (with preserved siderite-quartz-sulphide veins and associated Sn-W breccias). The oxidation state recorded by presence of ferric component in the tourmalines would have implications for Sn transport (as reduced Sn^{2+}) and precipitation as cassiterite on fluid oxidation (Taylor and Wall, 1992).

Age constraints for the tourmalinization event in the Val Trompia area are gained from the Rb-Sr radiometric cooling age of the Torgola Granite (271+/-4 Ma; De Capitani *et al.*, 1994) and by the observation that at Roccolo Pomo (fig. 2) the tourmalinization does not affect the Upper Permian Verrucano sandstones that are in tectonic contact along the reactivated Val Trompia Lineament.

It is difficult to correlate tourmalinization and granite intrusion with the large Torgola fluorite vein system (fig. 2). According to several workers (e.g., London and Manning, 1995), tourmalinization is most strongly developed in association with fluorine-rich granitic systems. In contrast, Pollard *et al.* (1987) distinguished between boron- and fluorine-rich systems, claiming that intense tourmalinization of host rocks is typical of B-rich, F-poor systems, which are also characterized by different styles of associated hydrothermal deposits. Our situation at Val Trompia is more compatible with Pollard's framework. Moreover, we do not see any connection between the tourmalinite and fluorite mineralization; the tourmalines are uniformly fluorine-poor, and no relationships are apparent between the fluorite mineralization and the Sn-W breccias (containing tourmalinite fragments). The fluorite veins cut the Torgola granite complex and the Upper Permian sandstones and therefore postdate the tourmalinization. Also, the Torgola granite complex is characterized by fluorine contents that do not exceed average values for normal granites (700 ppm F; De Capitani, unpubl. data).

A new contribution to knowledge of the Orobic tourmalinites is given by the data presented for coarse tourmaline crystals disseminated in the cryptocrystalline groundmass. The texture of the coarse tourmalines suggests that their crystallization predates the Alpine event: they record the

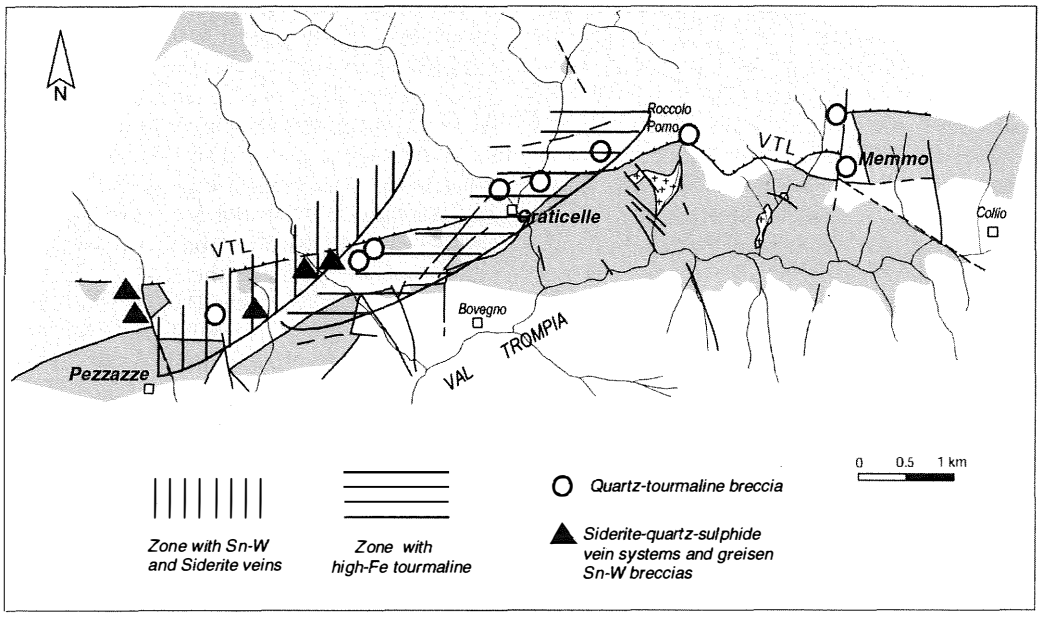

Fig. 10 – Zonal distribution of high-Fe tourmaline relative to granite outcrops and to siderite-quartz-sulphide vein deposits and associated Sn-W greisen breccias.

Alpine deformation by developing thin recrystallized rims and by producing pressure shadows oriented according to the Alpine mylonitic foliation. In these cataclasites the disseminated coarse tourmaline crystals and the fragments of undeformed, coarse tourmaline-rich vein quartz (sample T101) show a relatively homogeneous composition that distinguishes them from the foliation-concordant tourmaline enrichments in metamorphic basement clasts (sample C17). Exceptions are rare, such as the tourmaline crystal in sample T102B that has a composition like that of the Fe-rich data point in sample C17 (fig. 8*b*), which probably is a relic of metamorphic origin. As stated in the previous section, the overall composition of the coarse tourmaline grains in the groundmass and in the quartz vein fragment is comparable to that shown by the type II tourmalines in Val Trompia.

We could not determine the composition of the individual cryptocrystalline tourmaline grains in the groundmass. However on the basis of the geological, textural and analytical data presented, we propose a relationship between coarse and cryptocrystalline tourmalines involving a multi-stage tourmalinization process related to long-lived tectonic and volcanic activity along Permian strike-slip faults. According to this model, the first phase of tourmalinization occurred with the emplacement of tourmaline-bearing quartz veins within dilation zones along the basin-bounding shear zones. Remnants of these veins may be represented by fragments of quartz-tourmaline veins in conglomerates along the contact zones. Fault reactivation with deep cataclasis of wall rocks and continued input of boron-rich hydrothermal fluids then formed massive tourmaline aggregates with grain sizes compatible with that of the cataclasite. Development of tourmalinization in the Permian conglomerates rather than in the basement orthogneiss was interpreted by Zhang *et al.* (1994) as related to different degree of porosity

between the two rock types. Alternatively, the boron-rich fluids may have found a favourable Al-rich environment for tourmaline deposition preferentially in the cataclastic conglomerates because of the high content of aluminous phyllosilicate minerals in their matrix.

According to our interpretation, the gross compositional similarities between the type II (main-stage) Val Trompia and coarse-grained Lake Diavolo tourmalines may reflect similarities between the two tourmalinizing processes which can be considered basically coeval. Local chemical and paragenetic complexities are recorded in the Val Trompia tourmalinites (gradual change from schorl-dravite to highly Fe-enriched, possibly povondraite-type composition) as well as those from Novazza (transition from «internal» alkali-deficient to «external» schorl-dravite compositions; Fuchs and Maury, 1995). These complexities may record the interplay of various parameters (rapid variations of fluid composition, fluctuations in T, fluid pressure, pH, fO_2, etc.), characteristic of the zones most proximal to the fluid and heat source.

Considerations on the geological and structural setting of Val Trompia and the central Orobic Alps during Permian time suggest a genetic affinity between the Val Trompia and Orobic tourmalinites. Both are seen as products of a large-scale hydrothermal system coeval with upper Palaeozoic plutono-volcanic activity and tectonism, which was also responsible for the emplacement of various types of magmatic-hydrothermal deposits (Sn-W, U-Mo-Zn, Fe carbonates, sulphides, quartz). In this framework the Val Trompia tourmalinites should represent deeper levels of the system (fig. 11), and be closer to the shallow magma chamber (mildly alkaline, Al-rich, Torgola-type magma) that fed the volcanic edifices via deep-reaching fractures along which the Orobic tourmalinites and borosilicate alteration zones related to mineralization formed. This interpretation of a magmatic affinity for the Orobic tourmalinites is supported by their high Be contents, as reported by Slack *et al.* (1996).

Novazza-Val Vedello might represent the focus of the central Orobic volcanic-hydrothermal system. So the compositional differences between Lake Diavolo and Novazza tourmalines may be interpreted in terms of relative distance of the Lake Diavolo tourmalinites from the Novazza-Val Vedello caldera-related hydrothermal center, where, like at Val Trompia, tourmalinization is spatially related to ore deposition.

Temperature estimates based on sulphur isotope fractionation between cogenetic sulphides at Novazza are 300°C ± 40°C for the inner-zone sulphide mineralization that formed after the inner-zone tourmaline alteration, for which a temperature around 400°C was proposed by Fuchs and Maury (1995). Temperatures involved in the formation of tourmaline breccias at Val Trompia may have ranged between 400 and 500°C on the basis of relationships with the granite and with the greisen-type Sn-W mineralization, which are compatible with the temperature interval typical of this type of mineralization (e.g., Lehmann, 1990).

CONCLUDING REMARKS

Metasomatic tourmaline-rich rocks in different parts of the Southern Alpine Belt (at Val Trompia and in the central Orobic Alps) are related to geological, structural, and metallogenic features that developed during late Palaeozoic post-Variscan rifting. Tourmalinites from two areas are texturally different: phyllite breccias variably replaced by acicular tourmaline and quartz at Val Trompia and ultra-cataclasites of basement rocks and Lower Permian cover strata metasomatized by cryptocrystalline tourmaline in the Orobic Alps. Comparison of the chemical characteristics of tourmalines and tourmalinites, using data presented here and those in the literature, and evaluation of the geological, magmatic, and structural settings in which the Southern Alpine tourmalinites presumably formed, suggest a genetic link between the two types of occurrences.

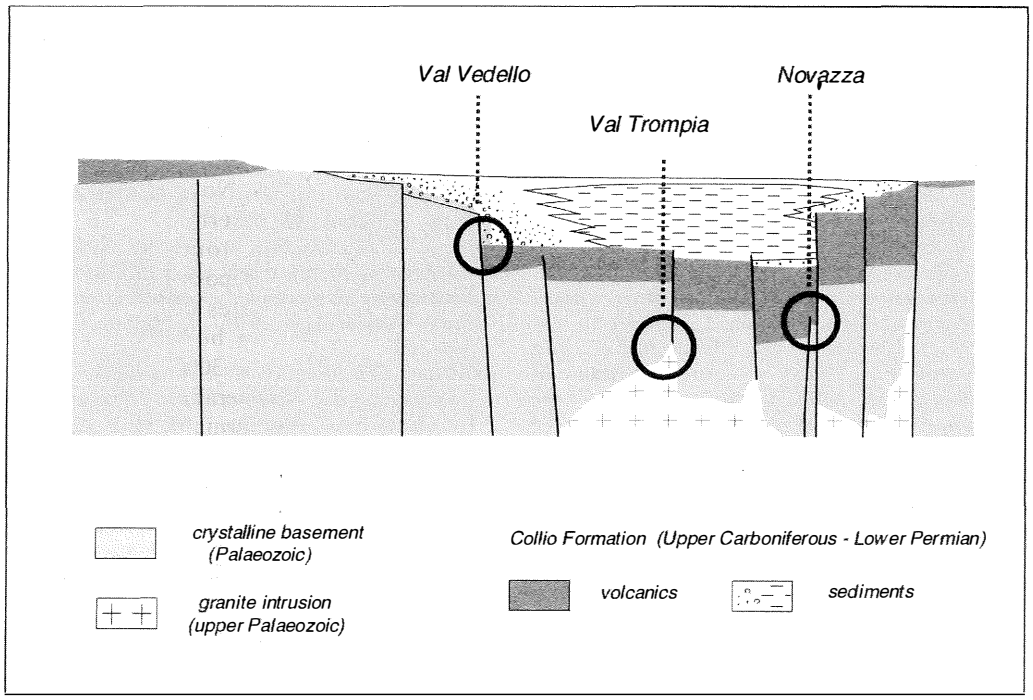

Fig. 11 – Position of the boron-bearing mineralized systems of Val Trompia and of the Orobic Alps (Novazza and Val Vedello) within the Collio rift system prior to Upper Permian (not to scale; modified after Cadel *et al.*, 1984).

Important information was gained by the investigations of the Val Trompia tourmalinites. The compositional variations of tourmaline in these granite-related quartz-tourmaline breccias help in distinguishing successive stages of tourmalinization, which record changing fluid conditions. The different chemical signatures of the host rocks undergoing metasomatism (basement schists) and of the magmatic fluids involved were preserved and recorded by the crystal chemistry and compositions of the tourmalines. Moreover, variations in the chemistry of the Val Trompia tourmalines, considered in relation to the distribution of the ore deposits, further confirms that tourmaline can be a valuable means for distinguishing different zones of a magmatic-hydrothermal mineralizing system exposed at different levels in the crust.

ACKNOLEDGEMENTS

The authors would like to thank Prof. Luciano Brigo for encouragement and Mr. Danilo Biondelli, Centro Studio Geodinamica Alpina e Quaternaria, Italian National Research Council, for assistance in ARL electron microprobe operations. The work was carried out with the financial support of M.U.R.S.T. (60%) of the University of Milano.

The authors are grateful to John Slack and Yves Fuchs for their constructive comments and reviews of the manuscript.

REFERENCES

AGAZZI S. (1997) — *Le tormaliniti al contatto Basamento-Copertura presso il Lago del Diavolo (Alta Val Brembana): aspetti geochimici, cristallochimici e confronti con altre tormaliniti del basamento.* Unpubl. Graduation thesis, Earth Science Dept., University of Milano, pp. 253.

ALDERTON D.H.M., PEARCE J.A. and POTTS P.J.

(1980) — *Rare Earth Element mobility during granite alteration: evidence from southwest England.* Earth Plan. Sci. Lett., **49**, 149-165.

ALLMAN-WARD P., HALLS C., RANKIN A. and BRISTOW C.M. (1982) — *An intrusive hydrothermal breccia body at Wheal Remfry in the western part of the St. Austell granite pluton, Cornwall, England.* In: Evans A.M. (Ed.), «Metallization associated with acid magmatism,» John Wiley and Sons, Chichester, 1-28.

CADEL G. (1986) — *Geology and uranium mineralization of the Collio Basin (central southern Alps, Italy).* Uranium, **2**, 215-240.

CADEL G., D'AGNOLO M., MENEGHEL L. and ZUFFARDI P. (1984) — *Polygenetism in stratiform/strata-bound uranium deposits of the Italian Alps.* In: «Proceedings of the 27th International geological Congress - Metallogenesis and Mineral Ore Deposits», **12**, 151-172.

CADEL G., FUCHS Y. and MENEGHEL L. (1987) — *Uranium mineralization associated with the evolution of a Permo-Carboniferous volcanic field. Examples from Novazza and Val Vedello (northern Italy).* Uranium, **3**, 407-421.

CADEL G., COSI M., PENNACCHIONI G. and SPALLA M.I. (1996) — A *new map of the Permo-Carboniferous cover and Variscan metamorphic basement in the central Orobic Alps, southern Alps, Italy: structural and stratigraphical data.* Mem. Sci. Geol., **48**, 1-53.

CASSINIS G. (1985) — *Il Permiano nel Gruppo dell'Adamello alla luce delle ricerche sui coevi terreni delle aree contermini.* Mem. Soc. Geol. It., **26**, 119-132.

CASSINIS G. and PEROTTI C.R. (1993) — *Interazione strutturale permiana tra la Linea delle Giudicarie ed i Bacini di Collio, Tione e Tregiovo (Sudalpino Centrale, N Italia).* Boll. Soc. Geol. It., **112**, 1021-1036.

CASSINIS G., FRIZZO P., MORONI M. and RODEGHIERO F. (1997) — *Le mineralizzazioni delle Alpi Bresciane: aspetti geologico-minerari e metallogenici.* In: Atti della Giornata di Studio «Le vene delle montagne», Brescia, 24 Novembre 1995, 139-148.

CAVARRETTA G. and PUXEDDU M. (1990) — *Schorl-dravite-ferridravite tourmalines deposited by hydrothermal magmatic fluids during early evolution of the Larderello geothermal field, Italy.* Econ. Geol., **85**, 1236-1251.

D'ANGIURO I. (1997) — *Le tormaliniti al contatto Basamento-Copertura affioranti a Sud del Lago di Publino (Alpi Orobie): caratteri cristallochimici e geochimici.* Unpubl. Graduation thesis, Earth Science Dept., University of Milano, pp. 221.

DE CAPITANI L. and MORONI M. (1992) — *Il microgabbro della Val Cavallina (Pezzaze, Prealpi Bresciane): caratteri chimici e mineralogici.* Rend. Fis. Acc. Lincei, **3**, 139-149

DE CAPITANI L., DELITALA G., LIBORIO G., MOTTANA A., RODEGHIERO F. and THÖNI M. (1994) — *The granitoid rocks of Val Navazze, Val Torgola and Val di Rango (Val Trompia, Lombardy, Italy).* Mem. Sci. Geol., **46**, 329-343.

DIELLA V., SPALLA M.I. and TUNESI A. (1992) — *Contrasting thermomechanical evolutions in the Southalpine metamorphic basement of the Orobic Alps (Central Alps, Italy).* J. Metam. Geol., 10, 202-219.

DINGWELL D.B., PICHAVANT M. and HOLTZ F. (1996) — *Experimental studies of boron in granitic melts.* In: Grew E.S., Anovitz L.M. (Eds.), «Boron: mineralogy, petrology and geochemistry». Reviews in Mineralogy, **33**, 331-385.

FOIT F.F. Jr. and ROSENBERG P.E. (1977) — *Coupled substitutions in the tourmaline group.* Contrib. Mineral. Petrol., **62**, 109-127.

FRIZZO P. (1997) — *Le mineralizzazioni a fluorite e solfuri polimetallici della Val Trompia.* In: Atti della Giornata di Studio «Le vene delle montagne», Brescia, 24 Novembre 1995, 149-163.

FUCHS Y., LAGACHE M. and LINARES J. (1998) — *Tourmaline synthesis under different T and $f(O_2)$ conditions.* Amer. Min., **83**, 525-534.

FUCHS Y. and MAURY R. (1995) — *Borosilicate alteration associated with U-Mo-Zn and Ag-Au-Zn deposits in volcanic rocks.* Mineral. Deposita, **30**, 449-459.

GALLAGHER V. (1988) — *Coupled substitutions in schorl-dravite tourmaline. New evidence from SE Ireland.* Mineral. Mag., **53**, 637-650.

GOSSO G., SILETTO G.B. and SPALLA M.I. (1997) — *HT/LP metamorphism and structures in the South Alpine basement near Lake Como, Orobic Alps; intracontinental imprints of the Permo-Triassic rifting.* Ofioliti, **22**, 133-145.

GIOBBI ORIGONI E. and GREGNANIN A. (1983) — *The crystalline basement of the «Massiccio delle Tre Valli Bresciane»: new petrographic and chemical data.* Mem. Soc. Geol. It., **26**, 133-144.

GREW E.S. and ANOVITZ L.M. (Eds.) (1996) — *Boron: mineralogy, petrology and geochemistry.* Reviews in Mineralogy, **33**, pp. 862, Mineralogical Society of America.

GRICE J.D. and ERCIT T.S. (1993) — *Ordering of Fe and Mg in the tourmaline crystal structure: the correct formula.* Neues Jahrb. Mineral. Abh., **165**, 245-266.

GRICE J.D., ERCIT T.S. and HAWTHORNE F.C. (1993) — *Povondraite, a redefinition of the tourmaline ferridravite.* Amer. Min., **78**, 433-436.

GRIECO G., DE CAPITANI L. and MORONI M. (in preparation) — *REE distribution in tourmalines related to Permian magmatism in Northern Italy: an ion probe investigation.*

HAWTHORNE F.C., MACDONALD D.J. and BURNS P.C. (1993) — *Reassignment of cation site occupancies in tourmaline: Al-Mg disorder in the crystal structure of dravite.* Amer. Min., **78**, 265-270.

HAWTHORNE F.C. and HENRY D.J. (1999) — *Classification of the minerals of the tourmaline group.* Eur. J. Mineral., **11**, 201-215.

HENRY D.J. and GUIDOTTI C.V. (1985) — *Tourmaline as a petrogenetic indicator mineral: an example from the staurolite-grade metapelites of NW Maine.* Am. Mineral., **70**, 1-15.

KING R.W., KERRICH R.W. and DADDAR R. (1988) — *REE distribution in tourmaline: an INAA technique involving pretreatment by B volatilization.* Am. Mineral., **73**, 424-431.

LEHMANN B. (1990) — *Metallogeny of Tin.* Lecture Notes in Earth Sciences, Volume **32**, Berlin, Springer-Verlag, pp. 211.

LONDON D. and MANNING D.A.C. (1995) — *Chemical variation and significance of tourmaline from southwest England.* Econ. Geol., **90**, 495-519.

LYNCH G. and ORTEGA J. (1997) — *Hydrothermal alteration and tourmaline-albite equilibria at the Coxheath porphyry Cu-Mo-Au deposit, Nova Scotia.* Can. Mineral., **35**, 79-94.

MACLEAN W.H. (1988) — *Rare earth element mobility at constant inter-REE ratios in the alteration zone at the Phelps Dodge massive sulphide deposit, Matagami, Quebec.* Mineral. Deposita, **23**, 231-238.

MILANO P.F., PENNACCHIONI G. and SPALLA M.I. (1988) — *Alpine and pre-Alpine tectonics in the central Orobic Alps (Southern Alps).* Eclog. Geol. Helv., **81**, 273-293.

MORA M.A. (1992) — *Caratteri geochimici e mineralogici del «granitoide» affiorante presso il Passo del Maniva (BS).* Unpubl. Graduation thesis, Earth Science Dept., University of Milano, pp. 122.

MORONI M. (1994) — *Identification of W-Sn mineralization associated with boron metasomatism in the crystalline basement of the Southern Italian Alps: preliminary observations on a new finding.* Chron. Rech. Min., **514**, 38-43.

NAKAMURA N. (1974) — *Determination of REE, Ba, Mg, Na, K in carbonaceous and ordinary chondrites.* Geoch. Cosmoch. Acta, **38**, 757-775.

ORI G.G., DALLA S. and CASSINIS G. (1986) — *Depositional history of the Permian continental sequence in the Val Trompia - Passo Croce Domini area (Brescian Alps, Italy).* Mem. Soc. Geol. It., **34**, 141-154.

PHILIPPE S., VILLEMAIRE C., LANCELOT J.R., GIROD M. and MERCADIER H. (1987) — *Données minéralogiques et isotopiques sur deux gîtes hydrothermaux uranifères du bassin volcano-sédimentaire permien de Collio Orobico (Alpes Bergamasques): mise en évindence d'une phase de remobilisation crétacée.* Bull. Mineral., **110**, 283-303.

POLLARD P.J., PICHAVANT M. and CHAROY B. (1987) — *Contrasting evolution of fluorine and boron-rich tin systems.* Mineral. Deposita, **22**, 315-321.

SLACK J.F. (1996) — *Tourmaline associations with hydrothermal ore deposits.* In: Grew E.S., Anovitz L.M. (Eds.), «Boron: mineralogy, petrology and geochemistry». Reviews in Mineralogy, **33**, 559-643.

SLACK J.F., HERRIMAN N., BARNES R.G. and PLIMER I.R. (1984) — *Stratiform tourmalinites in metamorphic terranes and their geologic significance.* Geology, **12**, 713-716.

SLACK J.F., PASSCHIER C.W. and ZHANG J.S. (1996) — *Metasomatic tourmalinite formation along basement-cover décollements, Orobic Alps, Italy.* Schweiz. Mineral. Petrogr. Mitt., **76**, 193-207.

TAYLOR J.R. and WALL V.J. (1992) — *The behavior of tin in granitoid magmas.* Econ. Geol., **87**, 403-420.

TAYLOR R.P. and FRYER B.J. (1982) — *Rare earth element geochemistry as an aid to interpreting hydrothermal ore deposits.* In: Evans A.M. (Ed.), «Metallization associated with acid magmatism,» John Wiley and Sons, Chichester, 357-365.

ZHANG J.S., PASSCHIER C.W., SLACK J.F., FLIERVOET T.F. and BOORDER H. DE (1994) — *Cryptocrystalline Permian tourmalinites of possible metasomatic origin in the Orobic Alps, northern Italy.* Econ. Geol., **89**, 391-396.